OXFORD GENETICS

GENETICS, 2022, 222(2), iyac120
https://doi.org/10.1093/genetics/iyac120
Advance Access Publication Date: 11 August 2022
Investigation
Highlighted Article

TOP-2 is differentially required for the proper maintenance of the cohesin subunit REC-8 on meiotic chromosomes in *Caenorhabditis elegans* spermatogenesis and oogenesis

Christine Rourke, Aimee Jaramillo-Lambert *

Department of Biological Sciences, University of Delaware, Newark, DE 19716, USA

*Corresponding author: Department of Biological Sciences, University of Delaware, 105 The Green, Newark, DE 19716, USA. Email: anjl@udel.edu

Abstract

During meiotic prophase I, accurate segregation of homologous chromosomes requires the establishment of chromosomes with a meiosis-specific architecture. The sister chromatid cohesin complex and the enzyme Topoisomerase II (TOP-2) are important components of meiotic chromosome architecture, but the relationship of these proteins in the context of meiotic chromosome segregation is poorly defined. Here, we analyzed the role of TOP-2 in the timely release of the sister chromatid cohesin subunit REC-8 during spermatogenesis and oogenesis of *Caenorhabditis elegans*. We show that there is a different requirement for TOP-2 in meiosis of spermatogenesis and oogenesis. The loss-of-function mutation *top-2(it7)* results in premature REC-8 removal in spermatogenesis, but not oogenesis. This correlates with a failure to maintain the HORMA-domain proteins HTP-1 and HTP-2 (HTP-1/2) on chromosome axes at diakinesis and mislocalization of the downstream components that control REC-8 release including Aurora B kinase. In oogenesis, *top-2(it7)* causes a delay in the localization of Aurora B to oocyte chromosomes but can be rescued through premature activation of the maturation promoting factor via knockdown of the inhibitor kinase WEE-1.3. The delay in Aurora B localization is associated with an increase in the length of diakinesis bivalents and *wee-1.3* RNAi mediated rescue of Aurora B localization in *top-2(it7)* is associated with a decrease in diakinesis bivalent length. Our results imply that the sex-specific effects of TOP-2 on REC-8 release are due to differences in the temporal regulation of meiosis and chromosome structure in late prophase I in spermatogenesis and oogenesis.

Keywords: *topoisomerase II*; TOP-2; REC-8; chromosome segregation; *Caenorhabditis elegans*; meiosis

Introduction

Accurate segregation of chromosomes to daughter cells during meiosis is essential for the maintenance of genomic stability between generations. Faithful segregation requires that meiotic chromosomes dramatically change in structure over the course of the meiotic program. Meiotic chromosome structural changes are mediated by the regulated association and dissociation of several protein complexes with chromosomes including cohesin complexes, the synaptonemal complex, and condensin complexes (Hillers *et al.* 2017).

During meiosis, chromosome axes conjoin linear looped arrays of sister chromatids at the loop base. Chromosome axes are composed of cohesin complexes, which are required for tethering sister chromatids together (sister chromatid cohesion or SCC), as well as meiosis-specific proteins such as the HORMA-domain proteins (Blat *et al.* 2002; Kim *et al.* 2014). In meiosis, the kleisin subunit of the cohesin complex is replaced with meiosis-specific subunits. In yeast, the meiosis-specific kleisin subunit is Rec8 (Rankin 2015). Higher eukaryotes have a Rec8 ortholog plus additional meiosis-specific kleisins including Rad21L in vertebrates and in *Caenorhabditis elegans*, the nearly identical COH-3 and COH-4 proteins (Klein *et al.* 1999; Pasierbek *et al.* 2001; Severson *et al.* 2009; Rankin 2015; Ishiguro 2019). In addition to establishing SCC, the meiosis-specific cohesin complexes serve as a basis for the assembly of the HORMA-domain proteins to axial elements. While yeast have a single meiosis-specific HORMA domain protein (Hop1), plants and mammals have 2 paralogs (ASY1/2 and HORMAD1/2, respectively), and *C. elegans* has 4 paralogs (HIM-3, HTP-1, HTP-2, and HTP-3; Hodgkin *et al.* 1979; Hollingsworth and Johnson 1993; Caryl *et al.* 2000; Pangas *et al.* 2004; Chen *et al.* 2005; Couteau and Zetka 2005; Goodyer *et al.* 2008; Wojtasz *et al.* 2009; Fukuda *et al.* 2010). These axis proteins are required for the assembly of the synaptonemal complex to establish homologous chromosome pairing, meiotic recombination, and meiotic checkpoint control thus, promoting proper chromosome segregation.

Also associated with meiotic chromosomes is the enzyme Topoisomerase II (TOP-2; Klein *et al.* 1992; Kleckner *et al.* 2013; Gómez *et al.* 2014; Mengoli *et al.* 2014; Jaramillo-Lambert *et al.* 2016). In mitosis of monocentric organisms, TOP-2 localizes to the chromosome axes (Earnshaw and Heck 1985; Gasser *et al.* 1986; Zickler and Kleckner 1999). In *C. elegans*, which have holocentric chromosomes, TOP-2 has a linear, exterior localization pattern on mitotic chromosomes that is distinct from the centromeres (Ladouceur *et al.* 2017). In meiosis, TOP-2 associates

Received: July 6, 2022. Accepted: August 1, 2022

diffusely with chromosomes during prophase (Moens and Earnshaw 1989; Klein *et al.* 1992; Cobb *et al.* 1999; Cheng *et al.* 2006; Zhang *et al.* 2014; Jaramillo-Lambert *et al.* 2016; Heldrich *et al.* 2020). Although TOP-2 is associated with meiotic chromosomes, its relationship between meiotic chromosome structure and meiotic axis components including cohesin and other axial elements is poorly understood.

The *C. elegans* genome contains a single gene that encodes for a TOP-2 ortholog, thus it is a genetically facile system for understanding the various functions of this enzyme. Previous work from our laboratory found that TOP-2 is differentially required for homologous chromosome segregation during meiosis I in male and female germlines (Jaramillo-Lambert *et al.* 2016). Analysis of *top-2(it7)*, a temperature-sensitive allele, in spermatogenesis showed that at the nonpermissive temperature (24°C) segregation of homologous chromosomes fails due to the formation of chromatin bridges at anaphase I. The meiotic divisions of oogenesis are not affected in the *top-2(it7)* mutant (24°C; Jaramillo-Lambert *et al.* 2016). TOP-2 is expressed throughout the germ lines of both spermatogenesis and oogenesis. TOP-2 associates with chromosomes in meiotic prophase (Jaramillo-Lambert *et al.* 2016). In *top-2(it7ts)* mutants, localization of TOP-2 is disrupted in both spermatogenesis and oogenesis, but chromosome segregation is only perturbed in spermatogenesis. Thus, the molecular mechanisms requiring differences in TOP-2 localization and/or activity at play in the 2 sexes are not known.

In this work, we study the sex-specific interdependent relationships between Aurora B kinase (AIR-2), REC-8, and TOP-2. We find that TOP-2 is differentially required in oogenesis and spermatogenesis to maintain the REC-8 cohesin subunit. When TOP-2 is disrupted during spermatogenesis, REC-8 is precociously removed at anaphase I. This is due to a failure to restrict the localization of Aurora B kinase and correlates with a failure to maintain the HORMA-domain proteins HTP-1 and HTP-2 (HTP-1/2) on chromosome axes after diakinesis. The disruption in HTP-1/2 localization leads to the mislocalization of downstream components that control Aurora B kinase localization. In contrast to spermatogenesis, loss of TOP-2 function during oogenesis neither disrupts HTP-1/2 localization nor most proteins that promote proper Aurora B localization. However, the localization of Aurora B to oocyte diakinesis chromosomes is delayed in a TOP-2 loss-of-function mutant. We propose that the sex-specific effects of TOP-2 on REC-8 release are due to differences in the temporal regulation of meiosis and chromosome structure in late prophase I in spermatogenesis and oogenesis.

Materials and methods

Strains

The following strains were maintained at 20°C under standard conditions, N2: wild-type Bristol strain, CB1489: *him-8(e1489)* IV, DG4915: *his-72(uge30)* III; *fog-2(oz40)* V, CV6: *lab-1(tm1791)/hT2* (de Carvalho *et al.* 2008), CV40: *rjIs1* [*Ppie-1 GFP::lab-1::HA; unc-119(+)*] (de Carvalho *et al.* 2008), AJL74: *rjIs1* [*Ppie-1 GFP::lab-1::HA; unc-119(+)*]; *him-8(e1489)* IV, and ATGSi23: *fqSi23* II *[Prec-8 rec-8: :GFP 3'UTR rec-8; cb-unc-119(+)]; rec-8(ok978)* IV (Ferrandiz *et al.* 2018). The remaining strains were maintained at 15°C under standard conditions and are as follows: AG259: *top-2(it7)* II; *him-8(e1489)* IV (Jaramillo-Lambert *et al.* 2016), AJL1: *top-2(ude1)* [it7 recreate] *fqSi23* [*Prec-8 rec-8::GFP 3'UTR rec-8; cb-unc-119(+)*] II; *rec-8(ok978)* IV. AJL73: *top-2(ude39)* [it7 recreate] II; *rjIs1* [*Ppie-1 GFP::lab-1::HA; unc-119(+)*]; *him-8(e1489)* IV.

Immunofluorescence and DAPI staining

Hermaphrodites and males were synchronized by picking L4s and incubating at 15°C for 16–24 h. Adult worms were then placed into a 24°C incubator for 4 h. For analysis of hermaphrodite spermatogenesis, L4 hermaphrodites were synchronized at the time of the 4-h incubation (Supplementary Fig. 2). Gonads were dissected in 30 µl of 1× Egg buffer (118 mM NaCl, 48 mM KCl, 2 mM $CaCl_2 \cdot 2H_2O$, 2 mM $MgCl_2 \cdot 6H_2O$, 25 mM HEPES, pH 7.4) and 0.1% Tween 20 on a glass coverslip. After dissection, 15 µl of liquid was removed and replaced with 15 µl 2% paraformaldehyde solution (16% paraformaldehyde from EM Sciences in 1× Egg buffer, 0.1% Tween 20). Fifteen microliters of liquid was removed and a Superfrost Plus microscope slide (Fisher, cat #12-550-15) was placed on top of the coverslip containing the dissected gonads. The slide and coverslip were flipped right-side up, allowed to fix for 5 min then placed into liquid nitrogen. Once frozen, the coverslip was quickly removed, and the slide was immediately submerged in −20°C methanol for 1 min. The slide was washed 3 times (5 min each) in PBST (1× PBS, 0.1% Tween 20). Following the 3 washes, the slides were incubated at room temperature for 1 h in a blocking solution (0.7% BSA in PBST). Fifty microliters of primary antibody diluted in blocking solution was placed on top of the gonads, covered with a parafilm coverslip, and incubated overnight (16–24 h) at room temperature in a humidified chamber. Following primary antibody incubation, slides were washed 3 times in PBST for 5 min each and incubated at room temperature with 50 µl of secondary antibody diluted in blocking solution in a humidified chamber for 2 h. Slides were washed 3 times for 5 min each in PBST, then stained with DAPI (2 µg/ml) for 5 min. Slides were washed for a final 5 min in PBST and mounted with Vectashield and a glass coverslip.

For experiments where DAPI staining alone was used, the worms were dissected, fixed, and frozen in liquid nitrogen as above. Once frozen, the coverslip was quickly removed, and the slide was immediately submerged in −20°C methanol for 1 min. The slide was washed 1 time (5 min) in PBST, removed, and incubated with DAPI (2 µg/ml) for 5 min in the dark. Slides were then washed for 5 min in PBST and mounted with Vectashield and a glass coverslip.

Primary antibodies used in this study were: rabbit anti-COH-3/4 (1:4000) (Severson and Meyer 2014), rabbit anti-REC-8 [(1:100) Fig. 1a] (Pasierbek *et al.* 2001), rabbit anti-HTP-1/2 (Martinez-Perez *et al.* 2008), guinea pig anti-HTP-3 (1:750) (MacQueen *et al.* 2005), rabbit anti-AIR-2 [(1:100) Figs. 2a and 6] (Schumacher *et al.* 1998), rabbit anti-AIR-2 [(1:500) Fig. 2c and Supplementary Fig. 2b] (Cell Signaling Technology, 2914S), Histone H3 phospho-T3 (1:750) (Millipore, 07-424), and rabbit anti-GFP [(1:500) Figs. 1c and 5, a and c; Supplementary Figs. 2a and 5a] (Novus Biologicals, NB600308). Secondary antibodies used were goat anti-rabbit Alexa Flour-568 and goat anti-guinea pig Alexa Flour-488 (1:200) (Invitrogen, Thermo Fisher Scientific, A11036 and A11073).

Image collection, processing, and measurements

Z-stack images of dissected gonads were obtained using a Zeiss LSM880 confocal microscope (Carl Zeiss, Inc., Gottingen, Germany) using a 63× objective and Zen software. For each gonad imaged, a full range of focal planes were selected to include the complete gonad, with a constant Z-step of 0.2 µm. Image processing and analysis were done using Fiji Is Just ImageJ [Fiji; Schindelin *et al.* 2012]. The range of focal planes used for z-stack projections in figures was chosen depending on the image and whether the image was of a male or a hermaphrodite gonad.

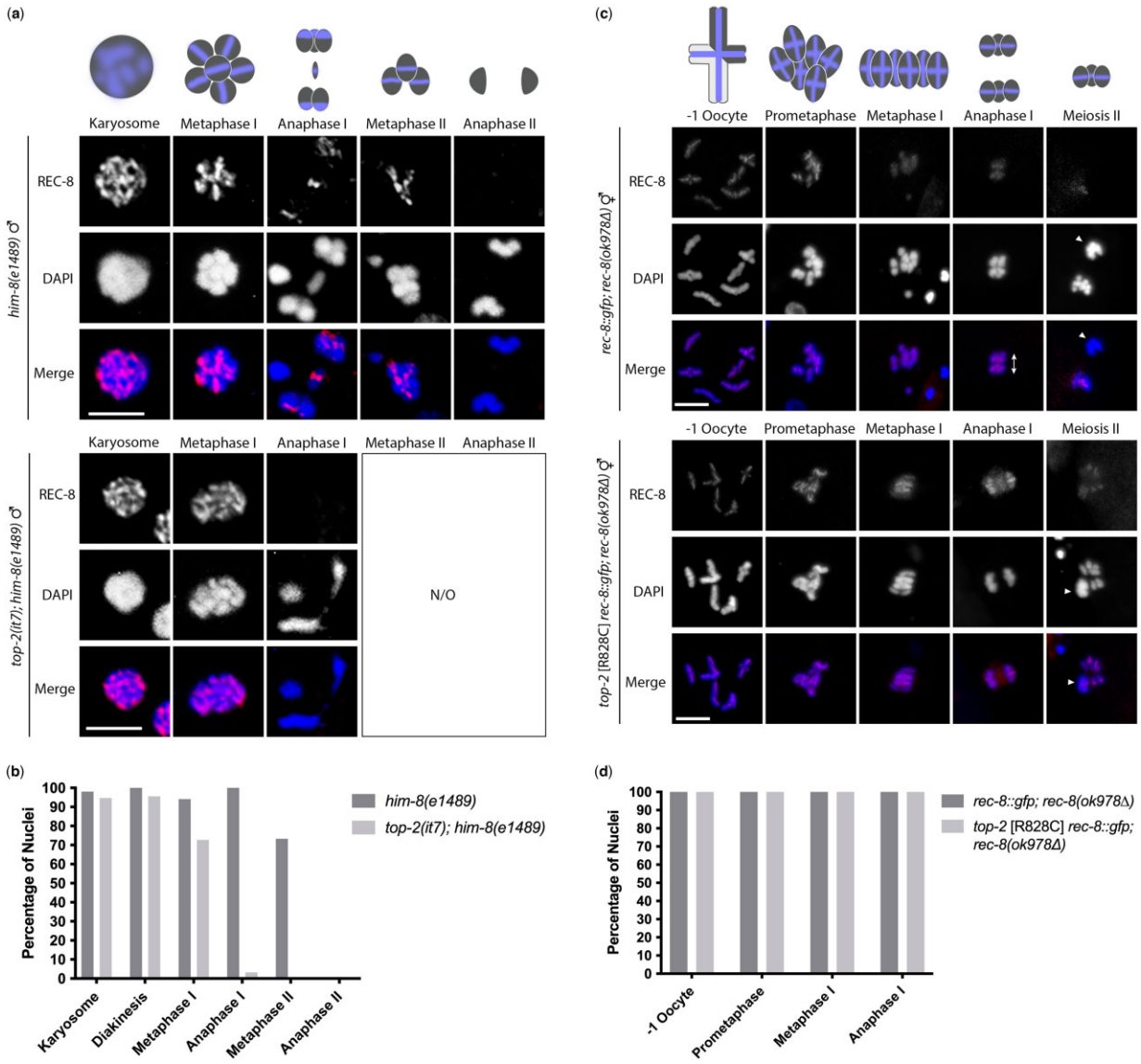

Fig. 1. REC-8 is prematurely removed from anaphase I meiotic chromosomes in *top-2(it7)* spermatogenic germlines but not oogenesis. Immunostaining of REC-8 (red) during spermatogenesis (a) and oogenesis (c) counterstained with DAPI (blue). a) Top: Schematic representation of chromosome morphology (dark gray) and REC-8 localization (periwinkle). Cross-sectional views of metaphase chromosomes show the bivalents as a "rosette" with the single X chromosome in the middle. During anaphase I, homologs separate to the spindle poles, while the X chromosome lags until it is eventually pulled to one of the poles. Bottom: Images are Z-projections of REC-8 (red) immunostaining in control [*him-8(e1489)*] and *top-2(it7); him-8(e1489)* during spermatogenesis nuclei from the karyosome through anaphase II. N/O = not observed. b) Quantification of nuclei positive for REC-8 staining in spermatogenesis. A total of 302 and 445 nuclei were examined from *him-8(e1489)* and *top-2(it7); him-8(e1489)*, respectively, from at least 3 biological replicates. c) Top: Schematic representation of chromosome morphology (light and dark gray) and REC-8 localization (periwinkle) in oogenesis. For ease of visualization, a single bivalent is indicated for diakinesis nuclei of the −1 oocyte. REC-8 localizes to both the short and long arm of bivalents in diakinesis through metaphase I. REC-8 is removed from the short arm of the bivalent prior to anaphase I for homolog segregation but remains localized between sister chromatids. REC-8 localizes between sister chromatids during meiosis II until it is removed at anaphase II for sister chromatid separation. Bottom: Z-projections of anti-GFP (red) immunostaining in *rec-8::gfp; rec-8(ok978Δ)* and *top-2* [R828C] *rec-8::gfp; rec-8(ok978Δ)* in oogenesis nuclei from the -1 oocyte through meiosis II. REC-8 localizes properly in *top-2* [R828C] *rec-8::gfp; rec-8(ok978Δ)* hermaphrodites. d) Quantification of nuclei positive for REC-8::GFP staining. A total of 46 and 30 oogenic nuclei were examined from *rec-8::gfp; rec-8(ok978Δ)* and *top-2* [R828C] *rec-8::gfp; rec-8(ok978Δ)*, respectively. At least 3 biological replicates were observed. Double-sided arrow in Anaphase I indicates direction of homolog segregation in this very early anaphase I nucleus. Arrowheads = polar body. Scale bars = 5 μm.

Images were taken using identical imaging parameters, but brightness and contrast were adjusted to allow for better visualization. Images used for bivalent length measurements were deconvolved using Huygens Profession 20.10 software. The deconvolved images were visualized in 3D using Imaris x64 9.7.2 software and measurements were made by visually delimiting individual diakinesis bivalents (Fig. 6d) and each bivalent length plotted using Prism (GraphPad Software).

RNAi

RNA was introduced into worms using the feeding method of Timmons *et al.* (2001). RNAi clones [*smd-1(F47G4.1)* and *wee-1.3(Y53C12A.1)*] were obtained from the OpenBiosytems ORF-RNAi library (Huntsville, AL). The *smd-1* RNAi construct was used as a negative control because it triggers the RNAi response, but produces no phenotypic effect (Boateng *et al.* 2017; Jaramillo-Lambert *et al.* 2015, 2016). Three to 5 L4 hermaphrodites were

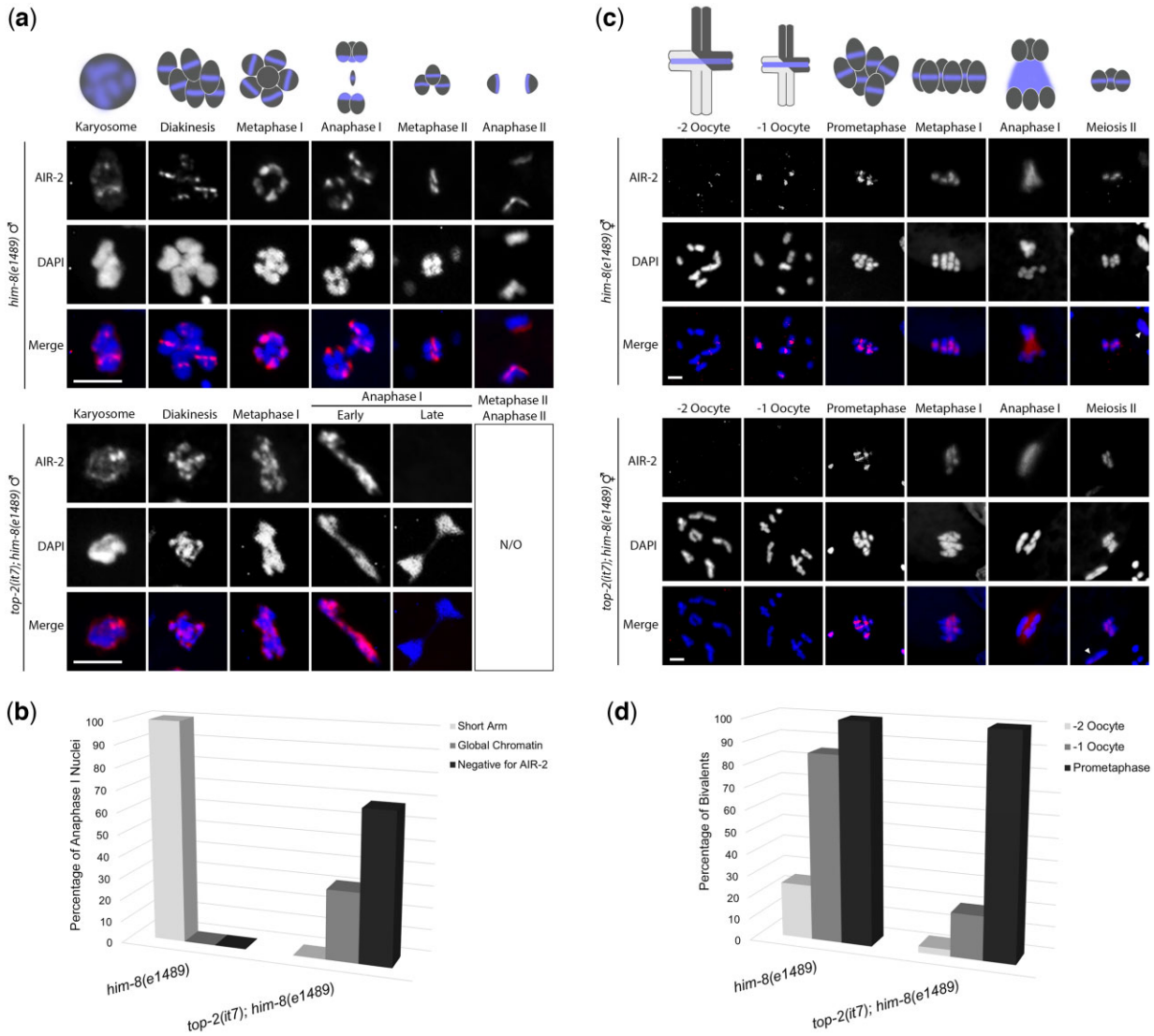

Fig. 2. TOP-2 is required for proper localization of AIR-2 during both oogenesis and spermatogenesis. Immunostaining of AIR-2 (red) in control [*him-8(e1489)*] and *top-2(it7); him-8(e1489)* spermatogenesis (a) and oogenesis (c) counterstained with DAPI (blue). a) Top: Schematic representation of chromosome morphology (dark gray) and AIR-2 localization (periwinkle). AIR-2 localizes to the short arm of bivalents in diakinesis through metaphase I (does not localize to the single X), is associated with the segregating chromosomes of anaphase I, and between sister chromatids during meiosis II (metaphase II and anaphase II). Bottom: Z-projections of karyosome through anaphase II nuclei in spermatogenesis. AIR-2 is localized to the DNA through anaphase II in control spermatogenesis. In *top-2(it7); him-8(e1489)* spermatogenesis AIR-2 is ectopically localized on anaphase I chromosomes. N/O = not observed. Scale bar = 5 μm. b) The quantification of the number of anaphase I nuclei either negative, short arm only, or ectopic [global chromatin] for AIR-2 localization during spermatogenesis in *him-8(e1489)* and *top-2(it7); him-8(e1489)*. A total of 20 and 63 anaphase I nuclei were examined from *him-8(e1489)* and *top-2(it7); him-8(e1489)*, respectively, from at least 3 biological replicates. c) Top: Schematic representation of chromosome morphology (light and dark gray) and AIR-2 localization (periwinkle). For ease of visualization, a single bivalent is indicated for diakinesis nuclei of the −2 and −1 oocytes. The size of the bivalent reflects the continued condensation of the bivalents as they prepare for the meiotic divisions. AIR-2 localizes to the short arm of bivalents in diakinesis through metaphase I, between segregating chromosomes of anaphase I, and between sister chromatids during meiosis II. Bottom: Z-projections of AIR-2 immunolocalization in oogenesis nuclei from the −1 oocyte through meiosis II. In *top-2(it7); him-8(e1489)*, AIR-2 is absent from the −1 oocyte, but localizes to chromosomes in prometaphase through metaphase of meiosis I, between segregating chromosomes of anaphase I and between sister chromatids of meiosis II nuclei. d) The quantification of the number of diakinesis bivalents displaying AIR-2 localization in the −2 and −1 oocytes and prometaphase I in *him-8(e1489)* and *top-2(it7); him-8(e1489)* oogenesis. One hundred and twenty-nine and 89 *him-8(e1489)* diakinesis bivalents were examined from the −1 and −2 oocytes, respectively. A total of 206 and 171 *top-2(it7); him-8(e1489)* diakinesis bivalents were examined from the −1 and −2 oocytes, respectively. One hundred and eight and 90 prometaphase bivalents were examined from *him-8(e1489)* and *top-2(it7); him-8(e1489)*, respectively. Overall, a total of 72 *him-8(e1489)* and 101 *top-2(it7); him-8(e1489)* oogenic nuclei were observed. A total of 17 *him-8(e1489)* and 23 *top-2(it7); him-8(e1489)* metaphase I through meiosis II single-cell embryos were observed. At least 3 biological replicates were examined. Arrowheads = polar body. Scale bar = 5 μm.

placed on a single 35 mm MYOB plate containing 1 mM IPTG (Roche, 11411446001) and 25 μg/ml carbenicillin and spotted with 50 μl of *Escherichia coli* HT115 [DE3] containing plasmids for RNAi knockdown. Hermaphrodites were allowed to lay embryos and 5 days post hatching (15°C) ∼20 L4 F1 progeny were transferred to fresh RNAi plates. After 16–24 h the F1 hermaphrodites were

transferred to 24°C for 4 h. After incubating at 24°C, worms were transferred to a glass coverslip for gonad dissection and immunostaining.

Embryonic viability mating assay

Single L4 males of the indicated genotype (Supplementary Fig. 5d) were mated with a single L4 *fog-2(oz40)* female at 20°C on an MYOB plate spotted with OP50 *E. coli*. Every 24 h the adult worms were transferred to fresh plates. This was repeated twice and on the third day, the adult male and female were discarded. The number of live progeny and dead embryos was counted for each 24-h period and the % embryonic viability was calculated. Three independent trials were performed for each mating assay. N2 male crosses $N = 20$ and *lab-1(tm1791)* $N = 22$.

CRISPR/Cas9-mediated genome editing

CRISPR-mediated genome editing to recreate the *top-2(it7)* R828C mutation in *fqSi23* [*prec-8; rec-8::gfp; rec-8 3'UTR; cb-unc-119(+)*] and *rjIs1* [*Ppie-1 GFP::lab-1::HA; unc-119(+)*] were done as in (Jaramillo-Lambert *et al.* 2016). A single line was generated carrying the R828C mutation in *fqSi23* and given the allele designation *ude1*. A single line carrying the R828C mutation in CV40 was given the allele designation *ude39*.

Results

TOP-2 is required to prevent the premature loss of the REC-8 subunit of cohesin in the male germline

We previously demonstrated through a time course analysis that TOP-2 functions late in meiotic prophase I of *C. elegans* around the time of major chromosome remodeling as the chromosomes prepare for segregation (Jaramillo-Lambert *et al.* 2016). To determine whether TOP-2 is required for chromosome remodeling and structural maintenance during late meiotic prophase, we examined the localization patterns of chromosome structural components in control [*him-8(e1489)*] and *top-2(it7); him-8(e1489)* male germlines at the nonpermissive temperature (24°C). *Caenorhabditis elegans* males have 5 pairs of autosomes and 1 sex chromosome (the X chromosome indicated as X0), which are observed as 6 DAPI staining bodies in wild type. Hermaphrodites have 5 pairs of autosomes and 1 pair of sex chromosomes (XX) (Corsi *et al.* 2015). The *him-8(e1489)* allele (**H**igh **I**ncidence of **M**ales) produces ~30% male progeny due to X chromosome nondisjunction facilitating assessment in males (Hodgkin *et al.* 1979; Phillips *et al.* 2005). Each homologous chromosome pair forms a single, asymmetrically placed crossover (CO), which divides the homolog pair into short and long segments (Albertson *et al.* 1997; Barnes *et al.* 1995; Nabeshima *et al.* 2005). In late meiotic prophase I (diplotene and diakinesis), the recombined homologous chromosomes are reorganized around the crossover site and condensed to form a cruciform structure with short and long arms (diakinesis bivalent; Chan *et al.* 2004). For the holocentric chromosomes of *C. elegans*, the CO site defines sister-chromatid co-orientation and where SCC will persist until anaphase II (long arm) [reviewed in Lui and Colaiácovo (2013)].

As previous work in a mammalian system found a link between Rec8 (chromosome structural component) removal and TOP-2 alpha decatenation activity (Gómez *et al.* 2014), we first examined the localization of the *C. elegans* meiosis-specific kleisin subunits of cohesin complexes, REC-8, COH-3, and COH-4. Although REC-8 and COH-3/COH-4 are all cohesin α-kleisin subunits, they make-up different cohesin complexes that are functionally distinct (Martinez-Perez *et al.* 2008; Severson *et al.* 2009; Severson and Meyer 2014). REC-8-containing cohesins becomes cohesive first during DNA replication while COH-3/4-containing cohesins do not become cohesive until the induction of meiotic double-strand breaks in early prophase I. Also, REC-8 co-orients sister chromatids during meiosis I and mediates SCC until anaphase II, while COH-3/4 cannot co-orient sister chromatids and only mediates cohesion until anaphase I (Severson and Meyer 2014). The analysis of localization using immunofluorescence in control [*him-8(e1489)*] males showed that REC-8 localized to the long arms of the bivalents at metaphase I through anaphase I and remained associated with sister chromatids until anaphase II (Fig. 1, a and b). In *top-2(it7); him-8(e1489)* spermatogenic germlines, we found that REC-8 localized to the chromosomes through metaphase I. A small percentage of metaphase I nuclei lacked REC-8 staining (~30% negative for REC-8) however, REC-8 was almost completely absent from the aberrant chromosome structures in anaphase I (96.8% negative for REC-8; Fig. 1, a and b). As previously demonstrated, no gross chromosome anomalies were observed in *top-2(it7)* from the start of meiosis (transition zone: leptotene and zygotene) through the karyosome (aggregation of paired homologous chromosomes into a single mass; Shakes *et al.* 2009). However, chromosome morphology is disrupted post karyosome at diakinesis through anaphase I and nuclei fail to proceed past anaphase I (Jaramillo-Lambert *et al.* 2016). We observed that while REC-8 localizes to metaphase I nuclei in *top-2(it7); him-8*, the chromosome structure is not wild type (Fig. 1a). Nonetheless, these data indicate that REC-8 is prematurely removed or lost from chromosomes during spermatogenesis of *top-2(it7)*.

Along with REC-8, *C. elegans* has 2 additional meiosis-specific kleisins, COH-3 and COH-4. COH-3 and COH-4 are 84% identical and are referred to as 1-unit COH-3/4 (Severson *et al.* 2009). During diakinesis of oogenesis, both COH-3/4 and REC-8 initially occupy both arms of the bivalent. At the diakinesis to metaphase I transition, COH-3/4 and REC-8 occupy different chromosomal domains of the bivalent, with COH-3/4 on the short arm and REC-8 on the long arm (Severson and Meyer 2014; Woglar *et al.* 2020). The examination of the meiotic divisions in spermatogenesis of *top-2(it7); him-8(e1489)* germlines (24°C) found that COH-3/4 localizes as foci in diakinesis and metaphase I of both *him-8(e1489)* and *top-2(it7); him-8(e1489)* (Supplementary Fig. 1). From these data, we conclude that TOP-2 is not disrupting COH-3/4 localization and focus on REC-8 for the remainder of this study.

To examine REC-8 localization in oogenesis, we used CRISPR/Cas9 genome editing to recreate the *top-2(it7)* mutation (R828C) in *fqSi23* II [*Prec-8 rec-8::GFP 3'UTR rec-8; cb-unc-119(+)*]; *rec-8(ok978)* IV. We will refer to this line as *top-2* [R828C] *rec-8::gfp; rec-8(ok978Δ)*. In diakinesis oocytes, REC-8 is found on both the long and short arm of the bivalents until late diakinesis or metaphase I when REC-8 is removed from the short arm (Rogers *et al.* 2002; de Carvalho *et al.* 2008; Harper *et al.* 2011; Severson and Meyer 2014; Ferrandiz *et al.* 2018). Using an anti-GFP antibody to determine REC-8::GFP localization, we confirmed that REC-8 localizes to both arms of diakinesis through metaphase I bivalents in control [*rec-8::gfp; rec-8(ok978Δ)*] oogenesis. REC-8 then localizes in between sister chromatids from anaphase I through metaphase II (Fig. 1, c and d). In *top-2* [R828C]; *rec-8::gfp; rec-8(ok978Δ)* oogenesis REC-8 had a similar localization pattern as observed in wild-type oogenesis. REC-8 localized to both arms of the bivalents in diakinesis through metaphase I and then between sister chromatids from anaphase I through meiosis II (Fig. 1, c and d). This

contrasted with the premature removal of REC-8 in *top-2(it7)* spermatogenesis consistent with the sperm-specific segregation defects of *top-2(it7)*.

To determine whether REC-8 mislocalization is spermatogenesis specific, we examined REC-8::GFP localization in hermaphrodite spermatogenesis, which occurs during larval development (Corsi *et al.* 2015). In control [*rec-8::gfp; rec-8(ok978Δ)*] hermaphrodite spermatogenesis REC-8::GFP localizes throughout the germline. At the karyosome and diakinesis stages, REC-8::GFP is found on the long arm of the bivalents where it remains through anaphase I. In meiosis II, REC-8::GFP remains associated with the sister chromatids until anaphase II when the sister chromatids separate (Supplementary Fig. 2a). This localization patterning is identical to the staining pattern we observed in control [*him-8(e1489)*] male spermatogenesis using a REC-8 antibody (Fig. 1a). In *top-2* [R828C] *rec-8::gfp; rec-8(ok978Δ)* hermaphrodite spermatogenesis, REC-8::GFP is associated with the chromosomes through metaphase I. REC-8::GFP was not observed on chromosomes of anaphase I nuclei (Supplementary Fig. 2a). These data confirm that mislocalization of REC-8 is a spermatogenesis-specific phenotype.

AIR-2 localization is redistributed in *top-2(it7)* mutants

In late meiotic prophase I, the Aurora B kinase, AIR-2, phosphorylates REC-8 marking it for removal from the bivalent short arms (Kaitna *et al.* 2002; Rogers *et al.* 2002; Severson and Meyer 2014; Ferrandiz *et al.* 2018). In meiosis II, AIR-2 marks REC-8 for removal from the sister chromatids. This 2-step mechanism of cohesin removal is accomplished through the spatial and temporal restriction of AIR-2, which is first found on the bivalent short arms during meiosis I and between sister chromatids in meiosis II (Rogers *et al.* 2002). Because REC-8 appears to be prematurely removed from chromosomes in *top-2(it7)* spermatogenic germlines and AIR-2 is responsible for marking REC-8 for removal, we investigated whether the localization of AIR-2 is disrupted in these germlines. As previously described (Shakes *et al.* 2009), AIR-2 localized to the external surface of karyosomes and then relocalized to the short arm of diakinesis bivalents in *him-8(e1489)* spermatogenesis (Fig. 2a). AIR-2 remains associated with segregating homologs during meiosis I, relocalizes between sister chromatids at metaphase II, and remains associated with the segregating chromosomes at anaphase II (Fig. 2a). AIR-2 association with segregating chromosomes in anaphase I is distinct from oogenesis, where AIR-2 localizes to the midzone of the meiotic spindle. In *top-2(it7); him-8(e1489)* spermatogenesis, AIR-2 was restricted to discrete areas of the chromosomes in the karyosome through metaphase I similar to controls. However, as chromosomes entered anaphase I, AIR-2 was ectopically localized with AIR-2 staining covering all regions of the chromosomes (Fig. 2, a and b). We define ectopic in this context as localization that is too broadly distributed; global chromatin localization rather than restricted to a distinct location. As the homologous chromosomes are unable to segregate in *top-2(it7); him-8(e1489)*, the chromosomes remain in an anaphase I configuration until the residual body is cleared (Jaramillo-Lambert *et al.* 2016). AIR-2 eventually disappears from the *top-2(it7); him-8(e1489)* anaphase I chromosomes (late anaphase I; Fig. 2, a and b).

We also examined whether ectopic localization of AIR-2 at anaphase I is spermatogenesis specific. Immunostaining assays were performed on spermatogenic germlines dissected from L4 control [*him-8(e1489)*] and *top-2(it7); him-8(e1489)* hermaphrodites. In *him-8(e1489)*, AIR-2 is on the short arm of the bivalent from diakinesis through metaphase I and then relocalizes to associate with the sister chromatids through anaphase II (Supplementary Fig. 2b). In *top-2(it7); him-8(e1489)* hermaphrodite spermatogenesis AIR-2 localizes to distinct regions of the chromatin from the karyosome until early anaphase I where it is ectopically localized on the chromatin. AIR-2 staining eventually disappears from late anaphase I structures similar to male spermatogenesis (Supplementary Fig. 2b). These results show that the *top-2(it7)*-induced ectopic localization of AIR-2 at anaphase I occurs during spermatogenesis of both hermaphrodites and males. The remainder of this study focuses on differences between male spermatogenesis and hermaphrodite oogenesis.

In diakinesis oocytes, AIR-2 localization is tightly regulated to restrict AIR-2 to the short arm of the bivalent of the 2 most proximal oocytes (−2 and −1 oocytes) and remains on the short arm through metaphase I. As we previously found that the *top-2(it7)* mutant did not disrupt chromosome segregation during oogenesis, we hypothesized that AIR-2 would localize to the bivalent short arm in *top-2(it7)* oogenic germlines. Surprisingly, we found that in *top-2(it7)* AIR-2 fails to localize to the −2 and −1 oocytes, however, it is present on prometaphase I through metaphase I chromosomes, at the spindle midzone of anaphase I, and between sister chromatids in meiosis II (Fig. 2, c and d). The "meiosis II" category consists of oocytes with a polar body and the remaining chromosomes in either prometaphase II, metaphase II, or anaphase II configuration. These results demonstrate that the loss of TOP-2 function disrupts at least 1 protein in the SCC pathway of oogenesis. However, the loss of TOP-2 function affects proteins required for homologous chromosome segregation differently in spermatogenesis and oogenesis.

TOP-2 is required for proper localization of SCC pathway proteins

Because the premature loss of REC-8 and ectopic localization of AIR-2 in *top-2(it7)* mutant spermatogenesis is reminiscent of defects in the SCC release pathway, we next examined the localization patterns of key SCC release components. In oogenesis, REC-8 removal is both spatially and temporally regulated by the SCC release pathway (de Carvalho *et al.* 2008; Ferrandiz *et al.* 2018). To determine if this was also true in spermatogenesis, we examined the localization patterns of the proteins involved in SCC release in the male germline.

In diakinesis oocytes Haspin-mediated phosphorylation of Histone H3 on threonine 3 (H3pT3) cues the recruitment of AIR-2 to the bivalent short arm (Ferrandiz *et al.* 2018). We next sought to determine if the ectopic localization of AIR-2 in anaphase I of *top-2(it7)* spermatogenic germlines was due to ectopic phosphorylation of Histone H3 threonine 3. During spermatogenesis, H3pT3 was detected at low levels starting at the karyosome stage with levels increasing through metaphase I (Fig. 3, a and b; Supplementary Fig. 3b). To help clarify the positional localization of H3pT3 on the diakinesis bivalents during spermatogenesis, we double stained the germlines with the chromosomal axis component HTP-3, which localizes to the meiotic chromosome axes and is found on both the long and short arms of diakinesis bivalents in oocytes (Goodyer *et al.* 2008; Severson *et al.* 2009). In control germlines [*him-8(e1489)*] HTP-3 localizes to chromosome axes of pachytene chromosomes through the early karyosome (Fig. 3a and Supplementary Fig. 3a). HTP-3 then disassociates from the chromosome axes as they progress through the condensation zone, until it reassociates on the long and short arms of the bivalents at diakinesis and metaphase I (Fig. 3a; Supplementary Fig. 3, b and c). The cross-shaped localization pattern of HTP-3 at

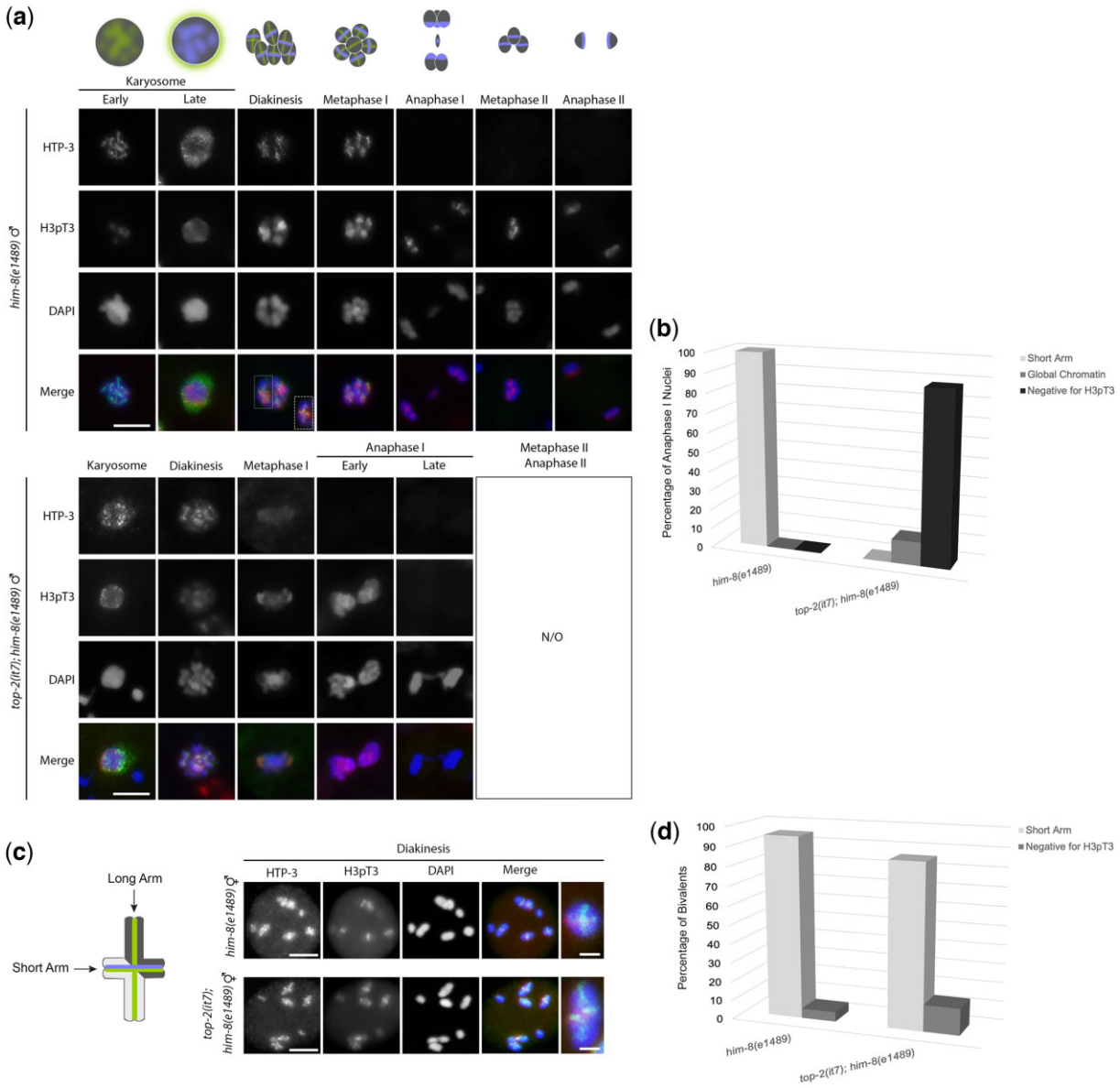

Fig. 3. TOP-2 is required for the proper localization of H3 T3 phosphorylation and HTP-3 during spermatogenesis. Immunostaining of H3pT3 (red) and HTP-3 (green) in control [*him-8(e1489)*] and *top-2(it7); him-8(e1489)* in spermatogenesis (a) and oogenesis (c), counterstained with DAPI (blue). a) Top: Schematic representation of HTP-3 (green) and H3pT3 (periwinkle) localization on chromosomes during spermatogenesis. Bottom: Z-projections of karyosome through anaphase II nuclei in spermatogenesis. H3pT3 localizes to the DNA at the karyosome where it remains through anaphase II in *him-8(e1489)* spermatogenesis. In *top-2(it7); him-8(e1489)* spermatogenesis H3pT3 loads properly at the karyosome but is ectopically localized at anaphase I. HTP-3 is localized to the chromosome axes at the karyosome, disassociates in the condensation zone, and reassociates with chromosomes at diakinesis where it remains through metaphase I in *him-8(e1489)* germlines. HTP-3 localization was detected in *top-2(it7); him-8(e1489)* spermatogenesis in the karyosome stage through metaphase I. A total of 194 *him-8(e1489)* and 288 *top-2(it7); him-8(e1489)* karyosome through anaphase II spermatogenic nuclei were examined. N/O = not observed. Scale bar = 5 μm. b) The quantification of the number of anaphase I nuclei either negative, short arm only, or ectopic [global chromatin] for H3pT3 localization during control [*him-8(e1489)*, $n = 155$] and *top-2(it7); him-8(e1489)* ($n = 155$) spermatogenesis. At least 3 biological replicates were examined. c) Left: Schematic representation of a diakinesis bivalent with HTP-3 (green) and H3pT3 (periwinkle) localization during oogenesis. Right: Z-projections of diakinesis nuclei in the −1 oocyte, and a single magnified bivalent in the last column. H3pT3 is localized to the short arm of diakinesis bivalents in the −1 oocyte in control and *top-2(it7); him-8(e1489)* animals. HTP-3 is localized to both the long and short arms of diakinesis bivalents in the −1 oocyte in *him-8(e1489)* and *top-2(it7); him-8(e1489)* animals. Scale bar = 5 μm. Magnified bivalent scale bar = 2 μm. d) The quantification of the number of diakinesis bivalents with H3pT3 localization on the short arm only, or negative for H3pT3 in either negative or short arm only. A total of 101 and 70 diakinesis bivalents were examined from *him-8(e1489)* and *top-2(it7); him-8(e1489)*, respectively, from at least 3 biological replicates.

diakinesis can be more clearly observed in the single-plane image (diakinesis inset). HTP-3 localization was no longer observed after metaphase I (Fig. 3a). Double staining of HTP-3 and H3pT3 showed that H3pT3 localizes to the short arm of the bivalent at diakinesis through metaphase I (Fig. 3a and Supplementary Fig. 3b). H3pT3 localization is also found associated with the chromosomes in anaphase I, between sister chromatids in metaphase II, and with segregating sister chromosomes at anaphase II (Fig. 3a).

In *top-2(it7); him-8(e1489)* spermatogenic germlines HTP-3 localizes to chromosome axes in pachytene (Supplementary Fig. 3a) but displays a disrupted chromosomal association in karyosome stage

nuclei. Following the karyosome stage, HTP-3 associates with the perturbed chromatin structures of diakinesis and metaphase I nuclei and is absent from anaphase I nuclei (Fig. 3a). In *top-2(it7); him-8(e1489)*, H3pT3 was found associated with chromosomes in the karyosome and diakinesis nuclei with some brighter H3pT3 foci at diakinesis. However, in metaphase I and anaphase I nuclei H3pT3 localization was disrupted. H3pT3 had an ectopic localization pattern on early anaphase structures and was absent from late anaphase I structures, similar to AIR-2 localization in *top-2(it7); him-8(e1489)* spermatogenic germlines (Fig. 3, a and b). From this, we believe that ectopic H3pT3 localization may contribute to the ectopic AIR-2 localization and thus the precocious removal of REC-8 in *top-2(it7)* mutant spermatogenesis.

We also examined the localization of HTP-3 and H3pT3 in *top-2(it7); him-8(e1489)* diakinesis oocytes. Neither HTP-3 nor H3pT3 localization was disrupted in the mutant germlines. HTP-3 localized to both the long and short arms of the diakinesis bivalents and H3pT3 localized to the short arms (Fig. 3, c and d; Supplementary Fig. 3d). Thus, *top-2(it7)* is not affecting timing of AIR-2 recruitment in oocytes at the level of H3 T3 phosphorylation.

The stepwise removal of cohesin in oogenesis is mediated through the spatiotemporal regulation of AIR-2, which in turn is regulated through the spatial recruitment of several proteins starting with the axis components HTP-1 and HTP-2 (82% identical and referred to as HTP-1/2; Martinez-Perez *et al.* 2008). The N-terminal domain of HTP-1/2 acts as a scaffold through LAB-1 to promote the recruitment of protein phosphatase 1 (PP1) to selectively dephosphorylate H3pT3 on the bivalent long arm (Ferrandiz *et al.* 2018). We next asked whether the localization of the scaffold proteins HTP-1/2 was disrupted in *top-2(it7)* mutant germlines. In control [*him-8(e1489)*] animals, we found that HTP-1/2 localized to the chromosomes in the transition zone (leptotene and zygotene) through pachytene and diakinesis in prophase I and then was lost from metaphase I chromosomes during spermatogenesis (Fig. 4, a and b; Supplementary Fig. 4). In *top-2(it7); him-8(e1489)* spermatogenic germlines, we found that HTP-1/2 localized to chromosomes similarly to control germlines in early stages of meiotic prophase I (Fig. 4, a and b; Supplementary Fig. 4). However, whereas HTP-1/2 was detected on 100% of diakinesis nuclei in control germlines, HTP-1/2 was undetectable in 50% of diakinesis nuclei in *top-2(it7); him-8(e1489)* germlines (Fig. 4, a and b). The examination of HTP-1/2 localization in both control [*him-8(e1489)*] and *top-2(it7); him-8(e1489)* oogenic germlines found that HTP-1/2 localizes to the diakinesis bivalent long arm (Fig. 4, c and d). These data indicate that TOP-2 is required to maintain HTP-1/2 localization during spermatogenesis, but not during oogenesis.

We also examined another component of the oocyte SCC release pathway in spermatogenesis, LAB-1. LAB-1 interacts with PP1 to restrict H3pT3 to the short arms of late diakinesis oocyte bivalents (de Carvalho *et al.* 2008; Ferrandiz *et al.* 2018). As LAB-1, which localizes to the long arms of oocyte bivalents, serves as the docking site for PP1 phosphatase, we asked if the ectopic localization of H3pT3 in spermatogenesis was due to either a failure to localize LAB-1 to chromosomes or mislocalization of the protein. To examine LAB-1 localization, we used a transgenic *C. elegans* strain with a GFP::LAB-1::HA fusion and performed immunostaining against GFP (de Carvalho *et al.* 2008). In control [GFP::LAB-1::HA; *him-8(e1489)*] spermatogenic germlines, GFP::LAB-1 was detected throughout meiotic prophase I (Fig. 5a and Supplementary Fig. 5a). GFP::LAB-1 chromosome tracks are detected throughout the karyosome and on diakinesis bivalents. GFP::LAB-1 begins to dissociate from the chromosomes at metaphase I (undetectable in ~22% of metaphase I nuclei) and is no longer detected at anaphase I through meiosis II (Fig. 5a). This is distinct from oogenesis where LAB-1 is detected in early meiotic prophase I (leptotene/zygotene) but remains associated with the chromosomes through early anaphase I (de Carvalho *et al.* 2008).

To examine LAB-1 localization in the context of the *top-2(it7)* mutation, we used CRISPR/Cas9 genome editing to recreate the *top-2(it7)* mutation (R828C) in *rjIs1* [*Ppie-1 GFP::lab-1::HA; unc-119(+)*] (de Carvalho *et al.* 2008) also containing the *him-8(e1489)* mutation. We will refer to this line as GFP::LAB-1::HA; *top-2* [R828C]; *him-8(e1489)*. In GFP::LAB-1::HA; *top-2* [R828C]; *him-8(e1489)* mutant spermatogenesis GFP::LAB-1 localizes to chromosomes in early meiotic prophase I similarly to the localization pattern observed in control germlines until metaphase I where GFP::LAB-1 is undetectable in the majority of metaphase I nuclei (15% positive for GFP::LAB-1, Fig. 5, a and b). The examination of the localization of LAB-1 in GFP::LAB-1::HA; *top-2* [R828C]; *him-8(e1489)* diakinesis oocytes found that GFP::LAB-1 localized to the long arm of the bivalents in the mutant germlines similar to control [GFP::LAB-1::HA; *him-8(e1489)*] germlines (Fig. 5, c and d).

As LAB-1 appears to have a sex-specific pattern of localization with LAB-1 disappearing earlier during spermatogenesis (metaphase I in spermatogenesis vs late anaphase I in oogenesis), it is possible that LAB-1 plays a distinct role in the SCC pathway during spermatogenesis from that of oogenesis. To determine if LAB-1 plays a role in SCC in spermatogenesis, we counted the number of DAPI staining bodies in diakinesis nuclei in *lab-1(tm1791)* mutant spermatogenic germlines. Analysis of *lab-1(tm1791)* worms revealed the presence of greater than 6 DAPI staining bodies in diakinesis spermatocytes (up to 10 DAPI staining bodies; Supplementary Fig. 5, b and c), which could be due to premature separation of homologous chromosomes or sister chromatids, defects in chromosome compaction, or chromosome fragmentation. However, mating *lab-1(tm1791)* males with *fog-2(oz40)* females did not result in a significant decrease in progeny viability [N2: 98.0%, *lab-1(tm1791)*: 91.8%, $P = 0.07$; Supplementary Fig. 5d] suggesting that although greater than 6 DAPI staining bodies are present, they are distributed correctly to make viable haploid gametes. This phenomenon has been previously documented in *C. elegans* and suggests that an achiasmate segregation mechanism is in place in male spermatogenesis (Jaramillo-Lambert *et al.*, 2010; Meneely *et al.* 2002). These data demonstrate that LAB-1 is involved in the proper pairing of homologous chromosomes during spermatogenesis. In addition, the GFP::LAB-1 immunostaining results are similar to the HTP-1/2 localization found in the *top-2(it7)* spermatogenic germlines suggesting that TOP-2 is required to maintain the localization of proteins that mediate SCC and its timely release.

Reduction of *wee-1.3* restores AIR-2 recruitment to diakinetic chromosomes

During oogenesis AIR-2 is not only regulated through restricted spatial recruitment to chromosomes, AIR-2 localization is also temporally regulated. Cyclin-dependent kinase (CDK-1) and cyclin B, as part of the maturation promoting factor (MPF), control the switch between diakinesis and metaphase I (Doree and Hunt 2002). In *C. elegans* oogenesis, CDK-1/MPF controls the timing of AIR-2 recruitment to the −2 and −1 oocytes (Ferrandiz *et al.* 2018). Wee1 kinase mediates the inhibition of Cdk1 through the phosphorylation of specific inhibitory sites (Doree and Hunt 2002). Thus, WEE-1.3 regulates the timing of AIR-2 recruitment to diakinesis bivalents through the inhibition of MPF (Ferrandiz *et al.*

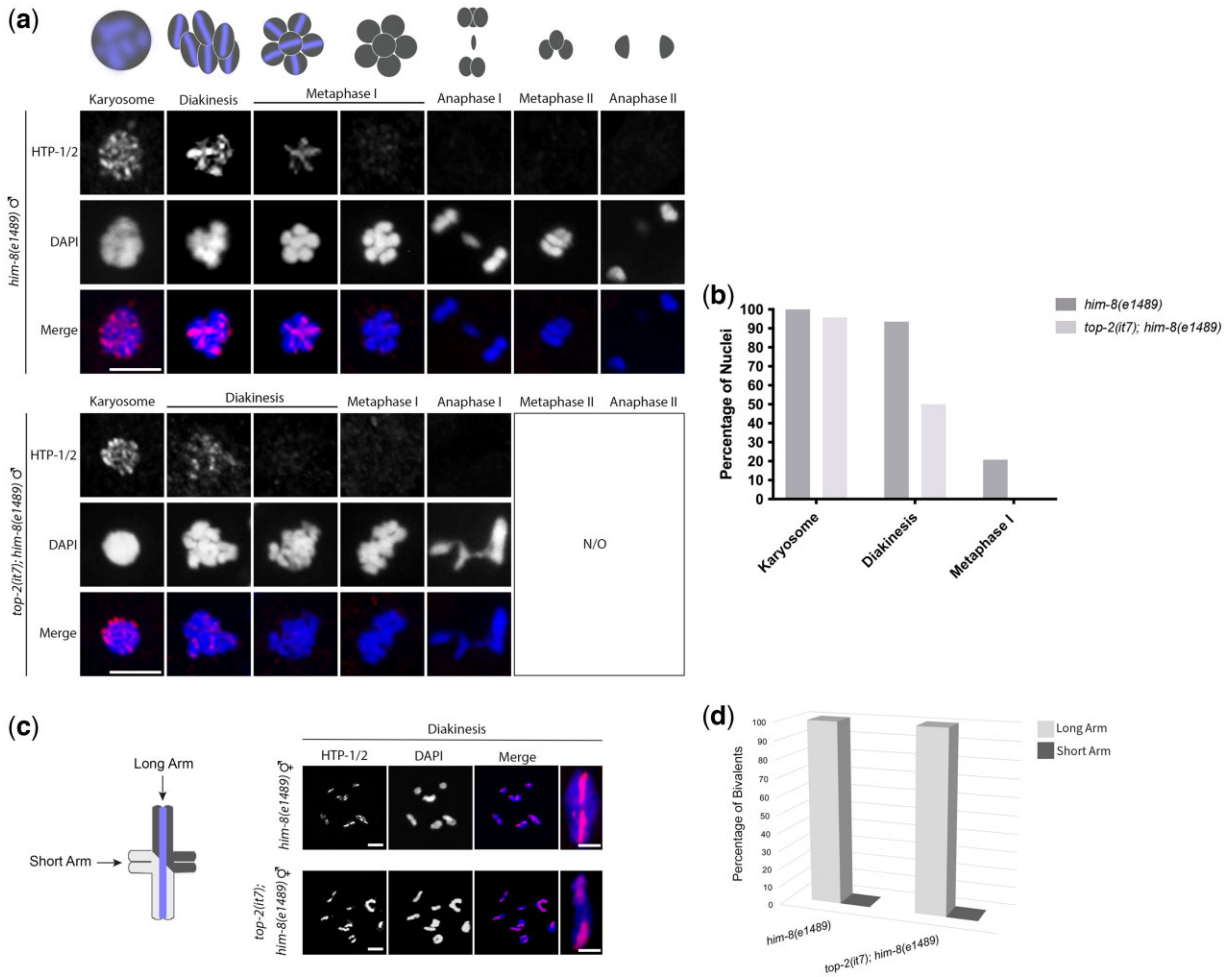

Fig. 4. TOP-2 is required for proper localization of HTP-1/2 during spermatogenesis, but not oogenesis. Immunostaining of HTP-1/2 (red) in control [*him-8(e1489)*] and *top-2(it7); him-8(e1489)* in spermatogenesis (a) and oogenesis (c), counterstained with DAPI (blue). a) Top: Schematic representation of chromosome morphology (dark gray) and HTP-1/2 localization (periwinkle) during spermatogenesis. Bottom: Z-projections of karyosome through anaphase II nuclei in spermatogenesis. In *him-8(e1489)* animals, HTP-1/2 is localized to the DNA through diakinesis stage nuclei and is removed at metaphase I. In *top-2(it7); him-8(e1489)* spermatogenesis, HTP-1/2 shows proper localization through the karyosome stage, however, it is prematurely removed at diakinesis. N/O = not observed. Scale bar = 5 μm. b) The quantification of the % nuclei positive for HTP-1/2 localization in the karyosome, diakinesis, and metaphase I of meiosis I during spermatogenesis. A total of 64 and 111 nuclei were examined from *him-8(e1489)* and *top-2(it7); him-8(e1489)*, respectively, from at least 3 biological replicates. c) Left: Schematic representation of a diakinesis bivalent with HTP-1/2 (periwinkle) localization during oogenesis. Right: Z-projections of HTP-1/2 localization at diakinesis in the −1 oocyte of *him-8(e1489)* and *top-2(it7); him-8(e1489)* oogenesis with a single magnified bivalent in the last column. Scale bar = 5 μm. Magnified bivalent scale bar = 2 μm. d) The quantification of the % bivalents with HTP-1/2 localization on the long arm or the short arm of diakinesis oocytes in both *him-8(e1489)* and *top-2(it7); him-8(e1489)*. A total of 62 and 87 diakinesis bivalents were examined from *him-8(e1489)* and *top-2(it7); him-8(e1489)*, respectively, from at least 3 biological replicates.

2018). As we observed a lack of AIR-2 staining in the −2 and −1 oocytes of *top-2(it7); him-8(e1489)* oogenic germlines, we investigated if the timing of AIR-2 localization could be restored in mutant germlines through inhibition of the WEE-1.3 kinase. Control RNAi (*smd-1*) recapitulated the *top-2(it7); him-8(e1489)* results; no detectable AIR-2 staining in -2 and -1 oocytes (Figs. 2 and 6, a and b). However, RNAi knockdown of *wee-1.3* restored AIR-2 localization to the bivalent short arm of *top-2(it7); him-8(e1489)* diakinesis chromosomes of the −1 oocytes (Fig. 6, a and b). This suggests that TOP-2 may help regulate the timing of AIR-2 recruitment during *C. elegans* oogenesis.

TOP-2 has been shown to be involved in chromosome condensation and in setting chromosome length in the soma (Nitiss 2009; Ladouceur *et al.* 2017). We reasoned that the *top-2(it7)* mediated disruptions to the localization of SCC pathway proteins could be due to disruptions in chromosome structure (condensation, length). Indeed, during the immunostaining experiments, it appeared that the diakinesis bivalents of *top-2(it7); him-8(e1489)* oocytes were longer than *him-8(e1489)* control oocytes. To determine if *top-2(it7)* affects bivalent length, we measured the lengths of individual diakinesis bivalents in *him-8(e1489)* vs *top-2(it7); him-8(e1489)* treated with control RNAi (*smd-1*). We found that bivalent length was increased in *top-2(it7); him-8(e1489) smd-1* RNAi compared to *him-8(e1489) smd-1* RNAi control (3.53 μm vs 2.95 μm, $P < 0.0001$, Fig. 6d). Depletion of *wee-1.3* via RNAi results in hypercompaction of oocyte bivalents [*him-8(e1489) smd-1* RNAi: 2.95 μm vs *him-8(e1489) wee-1.3* RNAi: 2.74 μm, $P < 0.01$; Fig. 6, c and d; Burrows *et al.* 2006 ; Allen *et al.* 2014]. This suggests that the rescue of AIR-2 localization in *top-2(it7); him-8(e1489)* oocytes depleted of *wee-1.3* could be due to changes in chromosome structure caused by the premature activation of the cell cycle. We measured the length of oocyte diakinesis bivalents in *top-2(it7); him-8(e1489)* treated with *smd-1* RNAi vs *wee-1.3* RNAi. Bivalent length was decreased in *top-2(it7); him-8(e1489) wee-1.3*

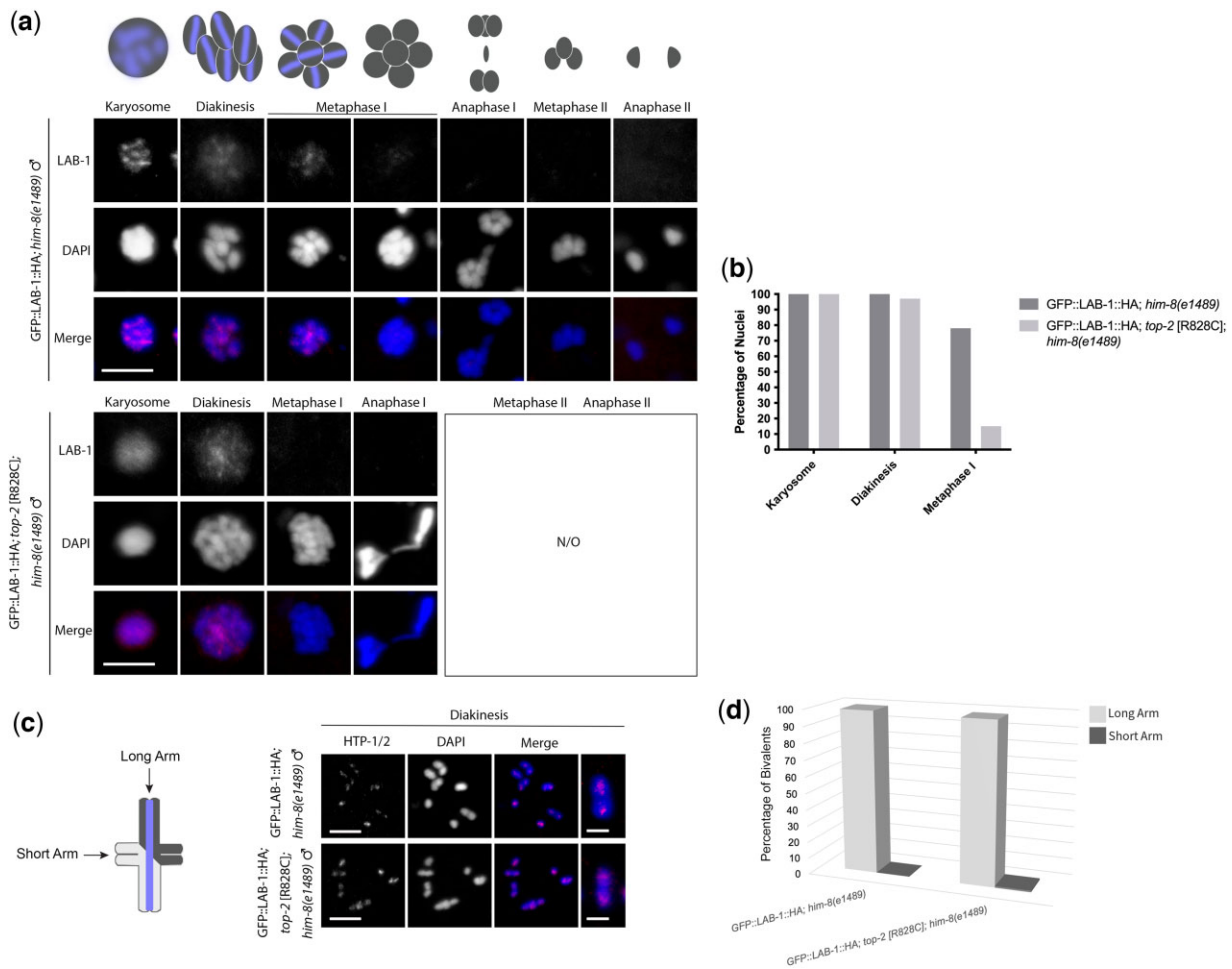

Fig. 5. TOP-2 is required for proper localization of LAB-1 during spermatogenesis, but not oogenesis. Immunostaining of GFP::LAB-1 (red) in control [GFP::LAB-1::HA; *him-8(e1489)*] and GFP::LAB-1::HA; *top-2* [R828C]; *him-8(e1489)* in spermatogenesis (a) and oogenesis (c), counterstained with DAPI (blue). a) Top: Schematic representation of chromosome morphology (dark gray) and LAB-1 localization (periwinkle) during spermatogenesis. Bottom: Z-projections of karyosome through anaphase II nuclei in spermatogenesis. In control animals GFP::LAB-1 is localized to the DNA at the karyosome and is removed by anaphase I. In GFP::LAB-1::HA; *top-2* [R828C]; *him-8(e1489)* animals GFP::LAB-1 is no longer detectable in metaphase I nuclei. A total of 308 GFP::LAB-1::HA; *him-8(e1489)* and 556 GFP::LAB-1::HA; *top-2* [R828C]; *him-8(e1489)* spermatogenic nuclei were examined. N/O = not observed. Scale bar = 5 μm. b) The quantification of the % nuclei positive for GFP::LAB-1 at the karyosome, diakinesis, and metaphase I stages of spermatogenesis. GFP::LAB-1::HA; *him-8(e1489)* metaphase I $n = 37$. GFP::LAB-1::HA; *top-2* [R828C]; *him-8(e1489)* $n = 54$. At least 3 biological replicates were examined. c) Left: Schematic representation of a diakinesis bivalent with LAB-1 (periwinkle) localization during oogenesis. Right: Z-projections of GFP::LAB-1 localization at diakinesis in the −1 oocyte of control [GFP::LAB-1::HA; *him-8(e1489)*] and GFP::LAB-1::HA; *top-2* [R828C]; *him-8(e1489)* animals. A single magnified bivalent is presented in the last column. LAB-1 localizes to the long arm in both control and GFP::LAB-1::HA; *top-2* [R828C]; *him-8(e1489)* diakinesis chromosome bivalents. Scale bar = 5 μm. Magnified bivalent scale bar = 2 μm. d) The quantification of the percentage of diakinesis bivalents with LAB-1 localization on the long arm or short arm. A total of 85 and 87 diakinesis bivalents were examined from GFP::LAB-1::HA; *him-8(e1489)* and GFP::LAB-1::HA; *top-2* [R828C]; *him-8(e1489)*, respectively, from at least 3 biological replicates.

RNAi (3.03 μm) vs *top-2(i7); him-8(e14890) smd-1* RNAi (3.53 μm; $P < 0.0001$; Fig. 6d). From these experiments, we conclude that TOP-2 is required for proper chromosome structure/bivalent length.

Discussion

The accurate segregation of homologous chromosomes during meiotic prophase I is a complex process. In meiotic prophase I, homologous chromosomes pair, synapse, and recombine. These intricate interactions require specific chromosome structures to be acquired at different points in the first meiotic prophase, which includes different chromatin conformations and the loading and unloading of specific proteins (condensins, cohesins, axial elements, and the synaptonemal complex). Our observation that a *top-2* hypomorphic mutation causes precocious loss of REC-8 from chromosomes during spermatogenesis prompted this investigation into the localization of chromosome structural components with a focus on proteins that regulate SCC release in the male germline. We found that the SCC release pathway components in *C. elegans* spermatogenesis have similar localization patterns to those in *C. elegans* oogenesis. At diakinesis, first the HORMA-domain proteins HTP-1/2, which localize along chromosome axes in pachytene, are redistributed to localize to the diakinesis bivalent long arm. We also found that the meiosis-specific cohesin subunit REC-8 localizes to the long arm of diakinesis bivalents. In contrast, COH-3/4 (additional meiosis-specific cohesin subunits), AIR-2, and H3 T3 phosphorylation are all found on the short arm of diakinesis bivalents. Interestingly, we found that LAB-1, the PP1 phosphatase binding partner, has a similar localization pattern in spermatogenesis as oogenesis but is removed from meiotic bivalents starting at metaphase I. This differs from

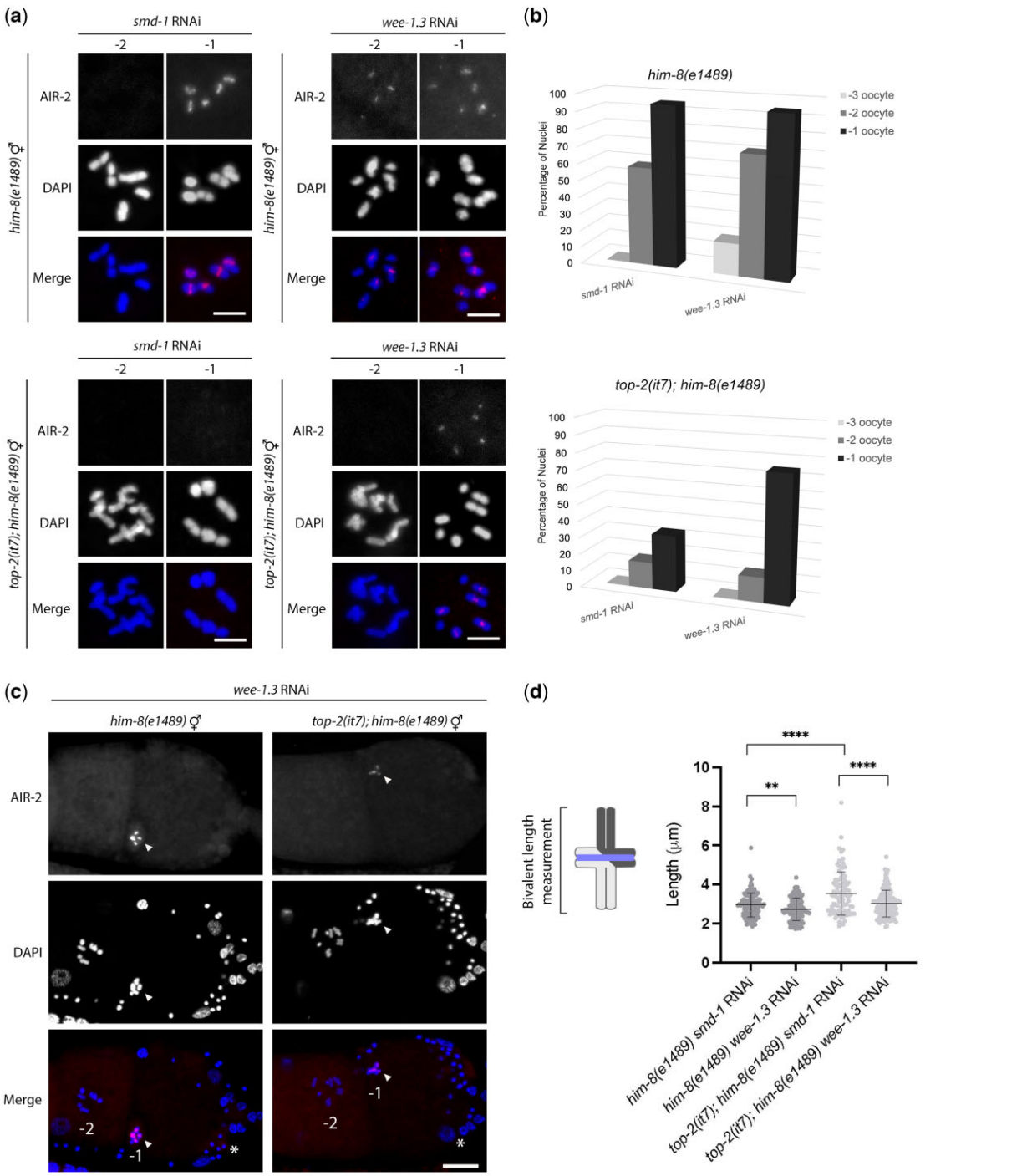

Fig. 6. Reduction of WEE-1.3 restores AIR-2 recruitment to diakinetic chromosomes during oogenesis. Immunostaining of AIR-2 (red) and DAPI (blue) in control [*him-8(e1489)*] and *top-2(it7); him-8(e1489)* treated with control and *wee-1.3* RNAi during oogenesis. a) Z-projections of −1 and −2 diakinesis oocytes, post-treatment with control RNAi [*smd-1*, left panels] or *wee-1.3* RNAi [right panels]. In control animals treated with *smd-1* RNAi, AIR-2 localizes to the short arm in the most proximal oocyte. Control worms treated with *wee-1.3* RNAi have precocious recruitment of AIR-2 in the −2 oocyte. *top-2(it7); him-8(e1489)* animals treated with *smd-1* RNAi fail to load AIR-2 to the short arm of diakinesis chromosome bivalents. *top-2(it7); him-8(e1489)* treated with *wee-1.3* RNAi restores AIR-2 localization to the −1 oocyte. b) The quantification of the percentage of nuclei with AIR-2 localization in the −1, −2, and −3 oocytes in control and *top-2(it7); him-8(e1489)* animals treated with *smd-1* or *wee-1.3* RNAi. A total of 72 −1, −2, and −3 oocyte nuclei were quantified for *him-8(e1489) smd-1* RNAi and a total of 53 −1, −2, and −3 oocyte nuclei were quantified for *him-8(e1489) wee-1.3* RNAi. A total of 57 −1, −2, and −3 oocyte nuclei were quantified for *top-2(it7); him-8(e1489) smd-1* RNAi and a total of 141 −1, −2, and −3 oocyte nuclei were quantified for *top-2(it7); him-8(e1489) wee-1.3* RNAi. At least 3 biological replicates were examined. c) Z-projection of the −1 and −2 oocytes in control and *top-2(it7); him-8(e1489)* worms treated with *wee-1.3* RNAi. Arrow points to the more condensed chromosome structure observed in *wee-1.3* depleted oocytes, and asterisks mark the spermatheca. d) Left: Schematic representation of a diakinesis bivalent with AIR-2 (periwinkle) localization on the short arm. Bivalent length was measured from one end of the long arm to the other end of the long arm (bracket). Right: Quantification of −1 oocyte bivalent length measurements in *him-8(e1489)* and *top-2(it7); him-8(e1489)* hermaphrodites treated with control (*smd-1*) or *wee-1.3* RNAi. Bivalent length is significantly decreased in *top-2(it7); him-8(e1489)* worms treated with *wee-1.3* RNAi when compared to control RNAi. The number of bivalents quantified is as follows: *him-8(e1489) smd-1* RNAi: $n = 115$, *him-8(e1489) wee-1.3* RNAi: $n = 114$, *top-2(it7); him-8(e1489) smd-1* RNAi: $n = 95$, *top-2(it7); him-8(e1489) wee-1.3* RNAi: $n = 135$. At least 3 biological replicates were analyzed. Statistical analysis was performed using a *t*-test. $^{****}P < 0.0001$, $^{**}P < 0.01$. Scale bar = 5 μm.

C. elegans oocytes, which maintain LAB-1 on the meiotic bivalents until late anaphase I. These findings reveal that while the localization of components required for the SCC release pathway is similar in spermatogenesis and oogenesis, the localization of these components in the male and female germline is not identical.

In addition to differences in the localization of SCC pathway proteins between oogenesis and spermatogenesis, this study revealed that the enzyme TOP-2 is differentially required for the localization of SCC pathway proteins in the germlines of males and females. The male germline is much more sensitive to a reduction in TOP-2 function. When males harboring a temperature-sensitive allele of *topoisomerase II*, *top-2(it7)*, were incubated at the nonpermissive temperature, several SCC release pathway components were disrupted. HTP-1/2 was prematurely removed from the long arms of diakinesis bivalents. This loss correlates with the ectopic localization of H3 T3 phosphorylation, ectopic AIR-2 localization, and the precocious removal of REC-8. Interestingly, the *top-2(it7)* mutant results in a unique phenotype, failure to segregate chromosomes at meiosis I, from what is observed in other mutants with ectopic localization of AIR-2 and precocious removal of REC-8. The Glc-7-like phosphatases GSP-1 and GSP-2 are required to both temporally and spatially restrict AIR-2 localization in *C. elegans* oogenesis. RNAi knockdown of these phosphatases results in AIR-2 localization both in more distal oocytes (up to −4 and −5) and in AIR-2 localization on both the short and long arms of diakinesis bivalents resulting in premature separation of chromosomes during meiosis I (Rogers *et al.* 2002; de Carvalho *et al.* 2008). The corresponding spermatogenesis-specific Glc-7-like phosphatases GSP-3 and GSP-4 are required for both chromosome segregation and sperm motility. The *gsp-3(tm1647) gsp-4(y418)* double mutant has a similar phenotype to *top-2(it7)* with the formation of chromatin bridges; however, the problem arises at anaphase II in *gsp-3(tm1647) gsp-4(y418)*, which results in both aneuploid and anucleate sperm, a phenotype distinct from *top-2(it7)*. The role of GSP-3 and GSP-4 in the SCC pathway has not been investigated, but the differences in phenotypes suggest that TOP-2 and the phosphatases have different roles in meiotic chromosome segregation.

In contrast to spermatogenesis, *top-2(it7)* oogenic germlines displayed normal localization of most SCC pathway components. The exception was AIR-2, which failed to localize to diakinesis oocytes, but was present on prometaphase I bivalent short arms. As homologous chromosomes prepare to segregate at anaphase of meiosis I, the chromosomes become highly condensed and restructured during late meiotic prophase to form the cruciform shape of the bivalent. Chromosome condensation and remodeling happen in both spermatogenesis and oogenesis, therefore, how does oogenesis compensate for the disrupted localization of AIR-2 in the *top-2* mutant and allow for accurate segregation of homologous chromosomes at meiosis I? One major difference between late meiotic prophase in oogenesis and spermatogenesis is timing of these events. In oogenesis, the transition from diakinesis to metaphase I is temporally regulated by the MPF. The MPF activates many hallmark events including nuclear envelope breakdown, rearrangement of the cortical cytoskeleton, and chromosome condensation and congression (Jones 2004; Von Stetina and Orr-Weaver 2011). In *top-2(it7)* mutants, we observed a lack of AIR-2 staining on −1 oocytes (diakinesis), but, surprisingly, AIR-2 was robustly localized to prometaphase I chromosomes (Fig. 2c). At this stage of the meiotic cell cycle, the chromosomes are in their most condensed configuration. Thus, we hypothesize that chromosome condensation state might also regulate the timing of AIR-2 localization (Fig. 7). Indeed, we found that knockdown of the MPF inhibitor kinase WEE-1.3, which results in precocious oocyte maturation including chromosome hypercondensation and congression (Burrows *et al.* 2006; Allen *et al.* 2014), restores AIR-2 localization to the −1 oocytes of *top-2(it7)* (Fig. 6, a and b). Our diakinesis bivalent length data also support this hypothesis. Oocyte diakinesis bivalent lengths are significantly increased in *top-2(it7); him-8(e1489); smd-1* RNAi compared to *him-8(e1489); smd-1* RNAi and AIR-2 localization is restored on the shorter bivalents of *top-2(it7); him-8(e1489); wee-1.3* RNAi (Fig. 6d). From these data, we propose that TOP-2 plays a role in chromosome structure in oogenic germlines, but relatively small disruptions caused by *top-2(it7)* can be compensated by later events of the diakinesis to metaphase transition (Fig. 7).

What is the link between TOP-2, chromosome structure, and the maintenance of HTP-1/2 localization in spermatogenesis?

In late meiotic prophase, chromosomes of both oocytes and spermatocytes resolve and condense as they prepare for the meiotic divisions. However, unlike oocytes which proceed from diakinesis to metaphase only after activation by MPF, spermatocytes proceed directly from diakinesis through the meiotic divisions (Chu and Shakes 2013). Another difference in meiotic prophase between oogenesis and spermatogenesis is that as spermatogenic chromosomes start to undergo chromatin remodeling in late prophase, the chromosomes condense and coalesce into a single mass called a karyosome (Shakes *et al.* 2009). It has been previously proposed that homologous chromosome compaction involves the cooperative actions of cohesins, condensins, and DNA topoisomerases (Kleckner 2006; Uhlmann 2016; Hillers *et al.* 2017; Cahoon and Libuda 2019). Our results support this hypothesis in spermatogenesis; loss of TOP-2 function in spermatogenesis leads to the premature loss of the meiotic cohesin subunit REC-8 (Fig. 1). However, *top-2(it7)* and *rec-8* mutants do not have identical phenotypes. We previously reported that *top-2(it7)* at the nonpermissive temperature leads to the formation of 100% anucleate sperm due to the formation of chromatin bridges at anaphase I that fail to segregate into budding sperm (Jaramillo-Lambert *et al.* 2016). In *rec-8* deletion mutants (*rec-8*Δ), sister chromatids separate at anaphase I (no crossovers are formed) in both oocytes and spermatocytes (Martinez-Perez *et al.* 2008; Severson *et al.* 2009). After meiosis I, the phenotypes of *rec-8* mutants differ between oocytes and sperm. In oocytes, there is neither a second chromosome segregation event nor cytokinesis leading to the formation of diploid gametes. In spermatogenesis, a second meiotic division does occur but both sets of chromosomes segregate to one spermatid (Roelens *et al.* 2015). The spermatocyte segregation defects of *rec-8*Δ resemble the *top-2(it7)* defects with abnormal anaphase structures, however, this occurs at anaphase II rather than anaphase I. One explanation for the difference could be that in the absence of REC-8, TOP-2 cannot perform its normal functions (decatenation) in meiosis II, while the earlier meiotic defect (anaphase I) observed in *top-2(it7)* is due to earlier requirements of TOP-2 in late meiotic prophase I (chromosome restructuring). This is in line with other organisms where TOP-2 and REC-8 occupy different locations on the chromosomes (general chromatin vs axes) and that loss of Rec8 in yeast does not impede the chromosomal accumulation of Top2 (Gómez *et al.* 2014; Heldrich *et al.* 2020).

We also found that the loss of REC-8 correlates with the upstream loss of the chromosome axis components HTP-1/2. How does loss of *top-2* function cause HTP-1/2 to be precociously lost

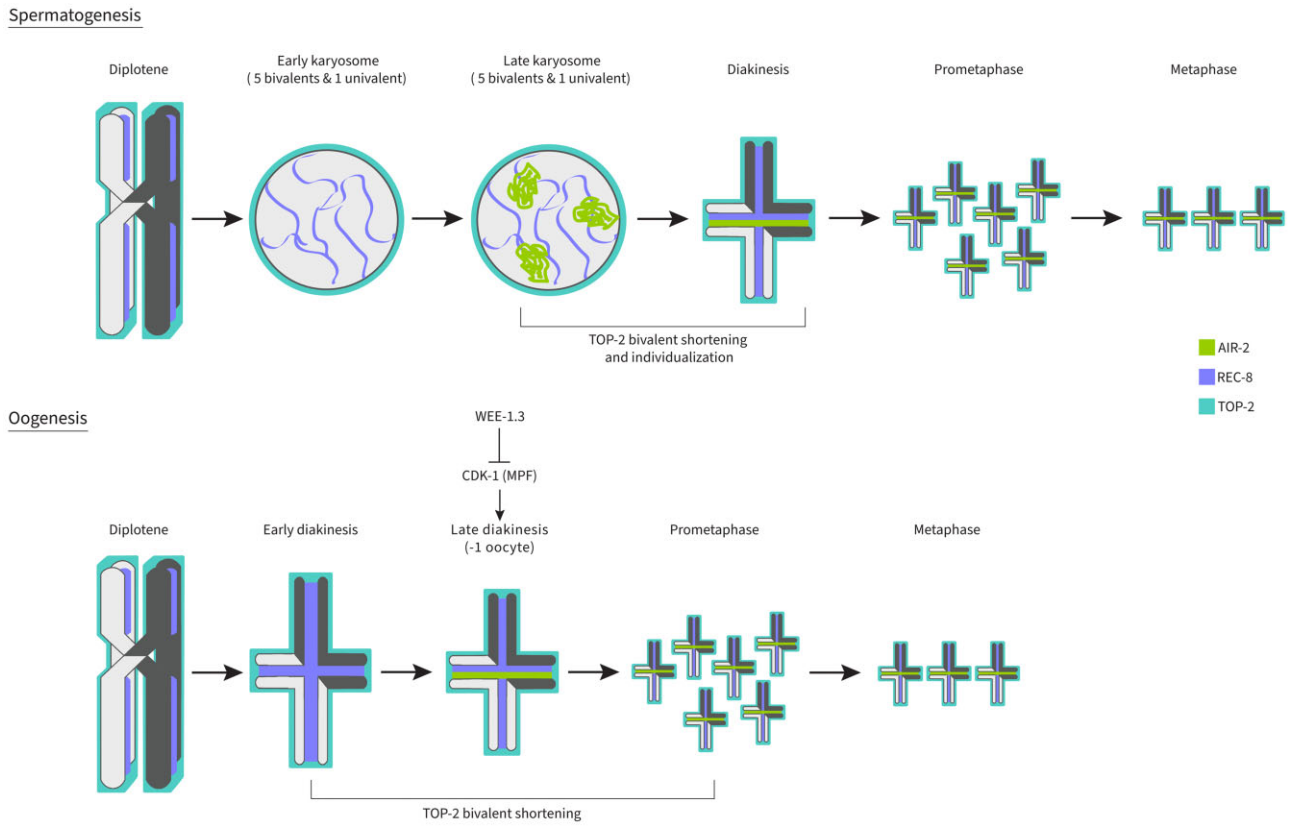

Fig. 7. Model of TOP-2 function in the events that control the release of REC-8 and chromosome remodeling in spermatogenesis and oogenesis. In both spermatogenesis and oogenesis TOP-2 (teal) localizes to chromatin. During spermatogenesis, TOP-2-mediated chromosome remodeling is required at the late karyosome to diakinesis transition to individualize and compact (shortening and condensation) the chromosomes. This allows for the proper maintenance of chromosome axis components (e.g. HTP-1/2, not depicted) and the subsequent regulation of the spatial localization of AIR-2 (green) to the short arm of diakinesis bivalents and the timely release of REC-8 (periwinkle). During oogenesis, TOP-2 functions at diakinesis through prometaphase I to mediate chromosome compaction (shortening and condensation). Once the chromosomes have reached the correct amount of compaction and in conjunction with the MPF, AIR-2 can be recruited to the short arms of the bivalents.

from meiotic chromosomes? We put forward the model that TOP-2-induced chromatin remodeling is required to prepare the chromosomes into a shape that promotes the continued binding of specific chromosome axis components (Fig. 7). Several examples in multiple organisms link TOP-2 and chromosome structure (Hartsuiker *et al.* 1998; Maeshima and Laemmli 2003; Xu and Manley 2007; Li *et al.* 2013; Hughes and Hawley 2014; Mengoli *et al.* 2014; Zhang *et al.* 2014; Liang *et al.* 2015). In addition, a connection between TOP-2 and meiotic axis components was demonstrated in budding yeast (Heldrich *et al.* 2020). In yeast, temperature-sensitive *top-2* mutants have delayed removal of the chromosome axis protein Hop1 (Heldrich *et al.* 2020). HTP-1/2 are homologs of yeast Hop1 (Zetka *et al.* 1999; Martinez-Perez and Villeneuve 2005). In contrast to budding yeast, we found that a temperature-sensitive *top-2* mutant leads to the early removal of HTP-1/2 from chromosomes in *C. elegans* spermatogenesis (Fig. 4). This is likely due to different mechanisms of homolog remodeling in yeast and worms. In budding yeast, Hop1 removal prior to SC assembly is required to recruit Pch2/TRIP13 for the remodeling of synapsed homologous chromosomes (Heldrich *et al.* 2020). In contrast, *C. elegans* HTP-1/2 are required to remain on chromosomes much later in meiotic prophase to promote the accurate localization of SCC release proteins. HTP-1/2 recruitment to chromosomes in early prophase is dependent on either binding axis proteins HTP-3 or HIM-3. HIM-3 is also dependent on HTP-3 for recruitment to chromosome axes (Kim *et al.* 2014). Unlike HTP-1/2, HTP-3 localizes to late prophase nuclei in *top-2(it7)* spermatogenesis (Fig. 3). One possibility is that TOP-2 directly binds to one or several of the axis proteins and loss of TOP-2 localization to chromosomes as in the *top-2(it7)* mutant (Jaramillo-Lambert *et al.* 2016) disrupts the localization of chromosome axis components. As disruption of HTP-1/2 and REC-8 localization was not observed in *top-2(it7)* oogenesis, we do not believe this is likely. Another possibility is that TOP-2 is required to help restructure the chromosomes as they emerge from the aggregated chromatin mass of the karyosome to become individualized entities of diakinesis nuclei. We believe this is the most plausible scenario. In *top-2(it7)* mutant spermatogenesis, chromosome structure appears grossly normal prior to the karyosome stage, but as the nuclei progress into diakinesis chromosome structure is severely disrupted in *top-2(it7)* mutant germlines with individual chromosome pairs indistinguishable from each other. Diakinesis chromosomes in oogenesis are also affected by the *top-2(it7)* mutant; bivalents are longer compared to controls. The more severe phenotype found in spermatogenesis (SCC protein mislocalization and chromosome segregation defects) is probably due to an increased requirement for TOP-2 in the karyosome to diakinesis transition (Fig. 7).

In this study, we focused on the role of TOP-2 and chromosome structural proteins in late meiotic prophase. While we cannot discount a role for TOP-2 in early meiotic events, we did not observe any obvious defects prior to late meiotic prophase with the *top-2(it7)*

mutant [this study and Jaramillo-Lambert *et al.* (2016)]. In the future, identification of new alleles or utilization of a degron-tagged TOP-2 protein may reveal roles for TOP-2 in early meiotic events as well. New alleles will also be useful in answering how loss of TOP-2 affects chromosome remodeling in late meiotic prophase in both spermatogenesis and oogenesis.

Data availability

Strains are available upon request. The authors state that all data necessary for confirming the conclusions are presented in the article and figures. Supplementary Fig. 1 shows the localization of COH-3/4 in male spermatogenesis. Supplementary Fig. 2 shows the localization of REC-8 and AIR-2 in hermaphrodite spermatogenesis. Supplementary Fig. 3 shows the dynamics of HTP-3 and H3pT3 localization in male spermatogenesis. Supplementary Fig. 4 shows HTP-1/2 localization in pachytene of male spermatogenesis. Supplementary Fig. 5 shows LAB-1 localization in pachytene and *lab-1* mutant defects in male spermatogenesis.

Supplemental material is available at *GENETICS* online.

Acknowledgments

The authors thank the following people for their gifts of antibodies: Jill Schumacher (AIR-2), Aaron Severson (COH-3/4), and Abby Dernburg (HTP-1/2 and HTP-3). They thank Monica Colaiacovo, Enrique Martinez-Perez, and David Greenstein for sharing strains. They also thank Amber Krauchunas and members of the Jaramillo-Lambert laboratory for critical reading of this manuscript.

Funding

Microscopy access was supported by grants from the NIH-NIGMS (P20 GM103446), the NSF (IIA-1301765), and the State of Delaware. The LSM880 confocal microscope was acquired with a shared instrumentation grant S10 OD016361. Some strains were provided by the CGC, which is funded by NIH Office of Research Infrastructure Programs (P40 0D010440). This work was supported by National Institutes of Health R03HD098244 and R35GM142524 (AJL). CR was supported by NIH T32GM133395 and a University of Delaware Graduate Scholars Award.

Conflicts of interest

None declared.

Literature cited

Albertson DG, Rose AM, Villeneuve AM. Chromosome organization, mitosis, and meiosis in C. elegans II. 2nd ed. Riddle DL, Blumenthal T, Meyer BJ, Priess JR, editors. New York (NY): Cold Spring Harbor; 1997.

Allen AK, Nesmith JE, Golden A. An RNAi-based suppressor screen identifies interactors of the Myt1 ortholog of Caenorha bditis elegans. G3 (Bethesda). 2014;4(12):2329–2343.

Barnes TM, Kohara Y, Coulson A, Hekimi S. Meiotic recombination, noncoding DNA and genomic organization in Caenorhabditis elegans. Genetics. 1995;141:159–179.

Boateng R, Nguyen KCQ, Hall DH, Golden A, Allen AK. Novel functions for the RNA-binding protein ETR-1 in *Caenorhabditis elegans* reproduction and engulfment of germline apoptotic cell corpses. Dev Biol. 2017;429(1):306–320.

Burrows AE, Sceurman BK, Kosinski ME, Richie CT, Sadler PL, Schumacher JM, Golden A. The *C. elegans* Myt1 ortholog is required for the proper timing of oocyte maturation. Development. 2006;133(4):697–709.

Cahoon CK, Libuda DE. Leagues of their own: sexually dimorphic features of meiotic prophase I. Chromosoma. 2019;128(3):199–214.

Caryl AP, Armstrong SJ, Jones GH, Franklin FC. A homologue of the yeast HOP1 gene is inactivated in the Arabidopsis meiotic mutant *asy1*. Chromosoma. 2000;109(1–2):62–71.

Chan RC, Severson AF, Meyer BJ. Condensin restructures chromosomes in preparation for meiotic divisions. J Cell Biol. 2004;167(4):613–625.

Chen YT, Venditti CA, Theiler G, Stevenson BJ, Iseli C, Gure AO, Jongeneel CV, Old LJ, Simpson AJG. Identification of CT46/HORMAD1, an immunogenic cancer/testis antigen encoding a putative meiosis-related protein. Cancer. Immun. 2005;5:9.

Cheng C-H, Lo Y-H, Liang S-S, Ti S-C, Lin F-M, Yeh C-H, Huang H-Y, Wang T-F. SUMO modifications control assembly of synaptonemal complex and polycomplex in meiosis of *Saccharomyces cerevisiae*. Genes Dev. 2006;20(15):2067–2081.

Chu DS, Shakes DC. Spermatogenesis. Adv Exp Med Biol. 2013;757:171–203.

Cobb J, Miyaike M, Kikuchi A, Handel MA. Meiotic events at the centromeric heterochromatin: Histone H3 phosphorylation, topoisomerase II alpha localization and chromosome condensation. Chromosoma. 1999;108(7):412–425.

Corsi AK, Wightman B, Chalfie M. A Transparent Window into Biology: A Primer on *Caenorhabditis elegans*. Genetics. 2015;200(2):387–407.

Couteau F, Zetka M. HTP-1 coordinates synaptonemal complex assembly with homolog alignment during meiosis in *C. elegans*. Genes Dev. 2005;19(22):2744–2756.

de Carvalho CE, Zaaijer S, Smolikov S, Gu Y, Schumacher JM, Colaiácovo MP. LAB-1 antagonizes the aurora B kinase in *C. elegans*. Genes Dev. 2008;22(20):2869–2885.

Doree M, Hunt T. From Cdc2 to Cdk1: when did the cell cycle kinase join its cyclin partner? J Cell Sci. 2002;115(Pt 12):2461–2464.

Earnshaw WC, Heck MM. Localization of topoisomerase II in mitotic chromosomes. J Cell Biol. 1985;100(5):1716–1725.

Ferrandiz N, Barroso C, Telecan O, Shao N, Kim HM, Testori S, Faull P, Cutillas P, Snijders AP, Colaiácovo MP, *et al.* Spatiotemporal regulation of aurora B recruitment ensures release of cohesion during *C. elegans* oocyte meiosis. Nat Commun. 2018;9:834–835.

Fukuda T, Daniel K, Wojtasz L, Toth A, Hoog C. A novel mammalian HORMA domain-containing protein, HORMAD1, preferentially associates with unsynapsed meiotic chromosomes. Exp Cell Res. 2010;316(2):158–171.

Gasser SM, Laroche T, Falquet J, Boy de la Tour E, Laemmli UK. Metaphase chromosome structure. Involvement of topoisomerase II. J Mol Biol. 1986;188(4):613–629.

Gómez R, Viera A, Berenguer I, Llano E, Pendás AM, Barbero JL, Kikuchi A, Suja JA. Cohesin removal precedes topoisomerase II alpha-dependent decatenation at centromeres in male mammalian meiosis II. Chromosoma. 2014;123(1–2):129–146.

Goodyer W, Kaitna S, Couteau F, Ward JD, Boulton SJ, Zetka M. HTP-3 links DSB formation with homolog pairing and crossing over during *C. elegans* meiosis. Dev Cell. 2008;14(2):263–274.

Harper NC, Rillo R, Jover-Gil S, Assaf ZJ, Bhalla N, Dernburg AF. Pairing centers recruit a polo-like kinase to orchestrate meiotic chromosome dynamics in *C. elegans*. Dev Cell. 2011;21(5):934–947.

Hartsuiker E, Bahler J, Kohli J. The role of topoisomerase II in meiotic chromosome condensation and segregation in *Schizosaccharomyces pombe*. Mol Biol Cell. 1998;9(10):2739–2750.

Heldrich J, Sun X, Vale-Silva LA, Markowitz TE, Hochwagen A. Topoisomerases modulate the timing of meiotic DNA breakage and chromosome morphogenesis in *Saccharomyces cerevisiae*. Genetics. 2020;215(1):59–73.

Hillers KJ, Jantsch V, Martinez-Perez E, Yanowitz JL. Meiosis. Worm Book. 2017;2017:1–43.

Hodgkin J, Horvitz HR, Brenner S. Nondisjunction mutants of the nematode *Caenorhabditis elegans*. Genetics. 1979;91(1):67–94.

Hollingsworth NM, Johnson AD. A conditional allele of the *Saccharomyces cerevisiae* HOP1 gene is suppressed by overexpression of two other meiosis-specific genes: RED1 and REC104. Genetics. 1993;133(4):785–797.

Hughes SE, Hawley RS. Topoisomerase II is required for the proper separation of heterochromatic regions during *Drosophila melanogaster* female meiosis. PLoS Genet. 2014;10(10):e1004650.

Ishiguro KI. The cohesin complex in mammalian meiosis. Genes Cells. 2019;24(1):6–30.

Jaramillo-Lambert A, Fuchsman AS, Fabritius AS, Smith HE, Golden A. Rapid and Efficient Identification of *Caenorhabditis elegans* Legacy Mutations Using Hawaiian SNP-Based Mapping and Whole-Genome Sequencing. G3 (Bethesda). 2015;5(5):1007–1019.

Jaramillo-Lambert A, Harigaya Y, Vitt J, Villeneuve A, Engebrecht J. Meiotic errors activate checkpoints that improve gamete quality without triggering apoptosis in male germ cells. Curr Biol. 2010; 20(23):2078–2089.

Jaramillo-Lambert A, Fabritius AS, Hansen TJ, Smith HE, Golden A. The identification of a novel mutant allele of topoisomerase II in *Caenorhabditis elegans* reveals a unique role in chromosome segregation during spermatogenesis. Genetics. 2016;204(4):1407–1422.

Jones KT. Turning it on and off: M-phase promoting factor during meiotic maturation and fertilization. Mol Hum Reprod. 2004; 10(1):1–5.

Kaitna S, Pasierbek P, Jantsch M, Loidl J, Glotzer M. The aurora B kinase AIR-2 regulates kinetochores during mitosis and is required for separation of homologous chromosomes during meiosis. Curr Biol. 2002;12(10):798–812.

Kim Y, Rosenberg SC, Kugel CL, Kostow N, Rog O, Davydov V, Su TY, Dernburg AF, Corbett KD. The chromosome axis controls meiotic events through a hierarchical assembly of HORMA domain proteins. Dev Cell. 2014;31(4):487–502.

Kleckner N. Chiasma formation: chromatin/axis interplay and the role(s) of the synaptonemal complex. Chromosoma. 2006;115(3): 175–194.

Kleckner N, Zickler D, Witz G. Molecular biology. Chromosome capture brings it all together. Science. 2013;342(6161):940–941.

Klein F, Laroche T, Cardenas ME, Hofmann JF, Schweizer D, Gasser SM. Localization of RAP1 and topoisomerase II in nuclei and meiotic chromosomes of yeast. J Cell Biol. 1992;117(5):935–948.

Klein F, Mahr P, Galova M, Buonomo SB, Michaelis C, Nairz K, Nasmyth K. A central role for cohesins in sister chromatid cohesion, formation of axial elements, and recombination during yeast meiosis. Cell. 1999;98(1):91–103.

Ladouceur A-M, Ranjan R, Smith L, Fadero T, Heppert J, Goldstein B, Maddox AS, Maddox PS. CENP-A and topoisomerase-II antagonistically affect chromosome length. J Cell Biol. 2017;216(9): 2645–2655.

Li X-M, Yu C, Wang Z-W, Zhang Y-L, Liu X-M, Zhou D, Sun Q-Y, Fan H-Y. DNA topoisomerase II is dispensable for oocyte meiotic resumption but is essential for meiotic chromosome condensation and separation in mice. Biol Reprod. 2013;89(5):118.

Liang Z, Zickler D, Prentiss M, Chang FS, Witz G, Maeshima K, Kleckner N. Chromosomes progress to metaphase in multiple discrete steps via global compaction/expansion cycles. Cell. 2015; 161(5):1124–1137.

Lui DY, Colaiácovo MP. Meiotic development in *Caenorhabditis elegans*. Adv Exp Med Biol. 2013;757:133–170.

MacQueen AJ, Phillips CM, Bhalla N, Weiser P, Villeneuve AM, Dernburg AF. Chromosome sites play dual roles to establish homologous synapsis during meiosis in *C. elegans*. Cell. 2005;123(6): 1037–1050.

Maeshima K, Laemmli UK. A two-step scaffolding model for mitotic chromosome assembly. Dev Cell. 2003;4(4):467–480.

Martinez-Perez E, Schvarzstein M, Barroso C, Lightfoot J, Dernburg AF, Villeneuve AM. Crossovers trigger a remodeling of meiotic chromosome axis composition that is linked to two-step loss of sister chromatid cohesion. Genes Dev. 2008;22(20):2886–2901.

Martinez-Perez E, Villeneuve AM. HTP-1-dependent constraints coordinate homolog pairing and synapsis and promote chiasma formation during *C. elegans meiosis*. Genes Dev. 2005;19(22): 2727–2743.

Meneely PM, Farago AF, Kauffman TM. Crossover distribution and high interference for both the X chromosome and an autosome during oogenesis and spermatogenesis in *Caenorhabditis elegans*. Genetics. 2002;162(3):1169–1177.

Mengoli V, Bucciarelli E, Lattao R, Piergentili R, Gatti M, Bonaccorsi S. The analysis of mutant alleles of different strength reveals multiple functions of topoisomerase 2 in regulation of *Drosophila* chromosome structure. PLoS Genet. 2014;10(10):e1004739.

Moens PB, Earnshaw WC. Anti-topoisomerase II recognizes meiotic chromosome cores. Chromosoma. 1989;98(5):317–322.

Nabeshima K, Villeneuve AM, Colaiácovo MP. Crossing over is coupled to late meiotic prophase bivalent differentiation through asymmetric disassembly of the SC. J Cell Biol. 2005;168(5): 683–689.

Nitiss JL. DNA topoisomerase II and its growing repertoire of biological functions. Nat Rev Cancer. 2009;9(5):327–337.

Pangas SA, Yan W, Matzuk MM, Rajkovic A. Restricted germ cell expression of a gene encoding a novel mammalian HORMA domain-containing protein. Gene Expr Patterns. 2004;5(2): 257–263.

Pasierbek P, Jantsch M, Melcher M, Schleiffer A, Schweizer D, Loidl J. A *Caenorhabditis elegans* cohesion protein with functions in meiotic chromosome pairing and disjunction. Genes Dev. 2001; 15(11):1349–1360.

Phillips CM, Wong C, Bhalla N, Carlton PM, Weiser P, Meneely PM, Dernburg AF. HIM-8 binds to the X chromosome pairing center and mediates chromosome-specific meiotic synapsis. Cell. 2005; 123(6):1051–1063.

Rankin S. Complex elaboration: making sense of meiotic cohesin dynamics. FEBS J. 2015;282(13):2426–2443.

Roelens B, Schvarzstein M, Villeneuve AM. Manipulation of karyotype in *Caenorhabditis elegans* reveals multiple inputs driving pairwise chromosome synapsis during meiosis. Genetics. 2015;201(4): 1363–1379.

Rogers E, Bishop JD, Waddle JA, Schumacher JM, Lin R. The aurora kinase AIR-2 functions in the release of chromosome cohesion in *Caenorhabditis elegans* meiosis. J Cell Biol. 2002;157(2):219–229.

Schindelin J, Arganda-Carreras I, Frise E, Kaynig V, Longair M, Pietzsch T, Preibisch S, Rueden C, Saalfeld S, Schmid B, *et al.* Fiji: an open-source platform for biological-image analysis. Nat Methods. 2012;9(7):676–682.

Schumacher JM, Golden A, Donovan PJ. AIR-2: an aurora/Ipl1-related protein kinase associated with chromosomes and midbody

microtubules is required for polar body extrusion and cytokinesis in *Caenorhabditis elegans* embryos. J Cell Biol. 1998;143(6):1635–1646.

Severson AF, Ling L, van Zuylen V, Meyer BJ. The axial element protein HTP-3 promotes cohesin loading and meiotic axis assembly in *C. elegans* to implement the meiotic program of chromosome segregation. Genes Dev. 2009;23(15):1763–1778.

Severson AF, Meyer BJ. Divergent kleisin subunits of cohesin specify mechanisms to tether and release meiotic chromosomes. Elife. 2014;3:e03467.

Shakes DC, Wu J-C, Sadler PL, Laprade K, Moore LL, Noritake A, Chu DS. Spermatogenesis-specific features of the meiotic program in *Caenorhabditis elegans*. PLoS Genet. 2009;5(8):e1000611.

Timmons L, Court DL, Fire A. Ingestion of bacterially expressed dsRNAs can produce specific and potent genetic interference in *Caenorhabditis elegans*. Gene. 2001;263(1–2):103–112.

Tzur YB, Egydio de Carvalho C, Nadarajan S, Van Bostelen I, Gu Y, Chu DS, Cheeseman IM, Colaiácovo MP. LAB-1 targets PP1 and restricts aurora B kinase upon entrance into meiosis to promote sister chromatid cohesion. PLoS Biol. 2012;10(8):e1001378.

Uhlmann F. SMC complexes: from DNA to chromosomes. Nat Rev Mol Cell Biol. 2016;17(7):399–412.

Von Stetina JR, Orr-Weaver TL. Developmental control of oocyte maturation and egg activation in metazoan models. Cold Spring Harb Perspect Biol. 2011;3(10):a005553.

Woglar A, Yamaya K, Roelens B, Boettiger A, Köhler S, Villeneuve AM. Quantitative cytogenetics reveals molecular stoichiometry and longitudinal organization of meiotic chromosome axes and loops. PLoS Biol. 2020;18(8):e3000817.

Wojtasz L, Daniel K, Roig I, Bolcun-Filas E, Xu H, Boonsanay V, Eckmann CR, Cooke HJ, Jasin M, Keeney S, *et al.* Mouse HORMAD1 and HORMAD2, two conserved meiotic chromosomal proteins, are depleted from synapsed chromosome axes with the help of TRIP13 AAA-ATPase. PLoS Genet. 2009;5(10):e1000702.

Xu YX, Manley JL. The prolyl isomerase Pin1 functions in mitotic chromosome condensation. Mol Cell. 2007;26(2):287–300.

Zetka MC, Kawasaki I, Strome S, Müller F. Synapsis and chiasma formation in *Caenorhabditis elegans* require HIM-3, a meiotic chromosome core component that functions in chromosome segregation. Genes Dev. 1999;13(17):2258–2270.

Zhang L, Wang S, Yin S, Hong S, Kim KP, Kleckner N. Topoisomerase II mediates meiotic crossover interference. Nature. 2014;511(7511):551–556.

Zickler D, Kleckner N. Meiotic chromosomes: integrating structure and function. Annu Rev Genet. 1999;33:603–754.

Communicating editor: J. Engebrecht